Computational and Structural Biotechnology Journal 23 (2024) 2358–2374

Contents lists available at ScienceDirect

Computational and Structural Biotechnology Journal

journal homepage: www.elsevier.com/locate/csbj

Research article

The complete catalog of antimicrobial resistance secondary active transporters in *Clostridioides difficile*: evolution and drug resistance perspective

Wannarat Chanket [a], Methinee Pipatthana [b], Apiwat Sangphukieo [c], Phurt Harnvoravongchai [d], Surang Chankhamhaengdecha [d], Tavan Janvilisri [e], Matthew Phanchana [f,*]

[a] *Graduate Program in Molecular Medicine, Faculty of Science, Mahidol University, Bangkok, Thailand*
[b] *Department of Microbiology, Faculty of Public Health, Mahidol University, Bangkok, Thailand*
[c] *Center of Multidisciplinary Technology for Advanced Medicine (CMUTEAM), Faculty of Medicine, Chiang Mai University, Chiang Mai, Thailand*
[d] *Department of Biology, Faculty of Science, Mahidol University, Bangkok, Thailand*
[e] *Department of Biochemistry, Faculty of Science, Mahidol University, Bangkok, Thailand*
[f] *Department of Molecular Tropical Medicine and Genetics, Faculty of Tropical Medicine, Mahidol University, Bangkok, Thailand*

ARTICLE INFO

Keywords:
Clostridioides difficile
Efflux pump
Secondary active transporter
Drug resistance
Gene expression
Structural similarity

ABSTRACT

Secondary active transporters shuttle substrates across eukaryotic and prokaryotic membranes, utilizing different electrochemical gradients. They are recognized as one of the antimicrobial efflux pumps among pathogens. While primary active transporters within the genome of *C. difficile* 630 have been completely cataloged, the systematical study of secondary active transporters remains incomplete. Here, we not only identify secondary active transporters but also disclose their evolution and role in drug resistance in *C. difficile* 630. Our analysis reveals that *C. difficile* 630 carries 147 secondary active transporters belonging to 27 (super)families. Notably, 50 (34%) of them potentially contribute to antimicrobial resistance (AMR). AMR-secondary active transporters are structurally classified into five (super)families: the *p*-aminobenzoyl-glutamate transporter (AbgT), drug/metabolite transporter (DMT) superfamily, major facilitator (MFS) superfamily, multidrug and toxic compound extrusion (MATE) family, and resistance-nodulation-division (RND) family. Surprisingly, complete RND genes found in *C. difficile* 630 are likely an evolutionary leftover from the common ancestor with the diderm. Through protein structure comparisons, we have potentially identified six novel AMR-secondary active transporters from DMT, MATE, and MFS (super)families. Pangenome analysis revealed that half of the AMR-secondary transporters are accessory genes, which indicates an important role in adaptive AMR function rather than innate physiological homeostasis. Gene expression profile firmly supports their ability to respond to a wide spectrum of antibiotics. Our findings highlight the evolution of AMR-secondary active transporters and their integral role in antibiotic responses. This marks AMR-secondary active transporters as interesting therapeutic targets to synergize with other antibiotic activity.

Abbreviations: AMR, antimicrobial resistance; AMR-secondary active transporters, antimicrobial resistance-associated secondary active transporters; AbgT, *p*-aminobenzoyl-glutamate transporter; DMT, drug/metabolite transporter superfamily; MATE, multidrug and toxic compound extrusion family; MFS, major facilitator superfamily; MOP, multidrug/oligosaccharidyl-lipid/polysaccharide flippase superfamily; PACE, proteobacterial antimicrobial compound efflux family; RND, resistance-nodulation-division family; SMR, small multidrug resistance family; CDI, *C. difficile* infection; FMT, fecal microbiota transplantation; BZX, bezlotoxumab (Zinplava); EP, efflux pump; ABC, ATP-binding cassette transporter; EPI, efflux pump inhibitor; AMX, amoxicillin; CIP, ciprofloxacin; CLI, clindamycin; CLO, cloxacillin; ERY, erythromycin; FDX, fidaxomicin; LMC, lincomycin; LVX, levofloxacin; MTZ, metronidazole; VAN, vancomycin.

* Correspondence to: Department of Molecular Tropical Medicine and Genetics, Faculty of Tropical Medicine, Mahidol University, 420/6 Ratchawithi Road, Ratchathewi, Bangkok 10400, Thailand.

E-mail address: matthew.pha@mahidol.ac.th (M. Phanchana).

https://doi.org/10.1016/j.csbj.2024.05.027
Received 8 February 2024; Received in revised form 1 May 2024; Accepted 16 May 2024
Available online 21 May 2024

1. Introduction

Clostridioides (*Clostridium*) *difficile* is a high risk pathogen due to its antibiotic resistance spectrum [1,2]. Exposure to broad-spectrum antibiotics (e.g., amoxicillin, ampicillin, cephalosporins, clindamycin, and fluoroquinolones) causes dysbiosis of gut microbiota. As a result, *C. difficile* can proliferate, colonize, and induce illness [3]. Pathogenicity of *C. difficile* infection (CDI) is caused by cytotoxin (TcdB) and/or enterotoxin (TcdA) [4]. TcdA and TcdB are glucosyltransferases that inactivate Rho family GTPase, which, in turn, disrupts the actin of epithelial cells and causes tight junction disruption, fluid secretion, epithelial cell rounding, and cell death [5]. Moreover, TcdA activates neutrophils causing an inflammatory response, while TcdB induces neutrophil chemotaxis and the formation of pseudomembranes [6]. Clinical manifestations of CDI range from mild diarrhea, severe diarrhea, pseudomembranous colitis, and megacolon to loss of life. As an obligate anaerobe, vegetative *C. difficile* cannot survive in an oxygenated environment. Therefore its dormant spore serves as an infective stage, primarily through the fecal-oral route. Currently, vancomycin (VAN) and fidaxomicin (FDX) are the primary antibiotics for CDI treatment [7,8]. Other antibiotics are ineffective for CDI due to intrinsic resistance mechanisms, such as an active efflux of antibiotics [9]. Recently, Bezlotoxumab, a monoclonal antibody that targets TcdB, received approval by the US FDA to mitigate the risk of CDI recurrence episodes in immunosuppressed patients or those who had severe, initial episodes. [10–12]. Additionally, fecal microbiota transplantation (FMT) is prescribed for patients with a history of multiple recurrence episodes. [13]. Monoclonal antibodies and FMT are reserved for treatment after multiple episodes and severe symptoms [14]. Antibiotics are still standard for initial infection and first recurrent episodes [8]. Therefore, advanced developments are centered around small molecule antibiotics [15]. Strategies to enhance or retain antibiotic activity remain the focus of current research (e.g., an approach counteracting resistance mechanisms by preventing drug extrusion, allowing them to reach their target).

Efflux pumps (EPs) are transmembrane proteins that function as active exporters of antibiotic(s) from within the cell, contributing to antimicrobial resistance (AMR) [16]. Active transporters are classified into 2 types: primary active transporters energized by ATP hydrolysis and secondary active transporters, which utilize force from an electrochemical gradient of solutes [17]. ATP-binding cassette (ABC) transporters, known as primary active transporters are ubiquitous in all domains of life, serving as both importers and exporters. ABC subfamily III, VI, VII, and IX have been shown to contribute to multidrug resistance in *C. difficile* [18,19]. In addition, four groups of secondary active transporters have been associated with drug resistance: major facilitator superfamily (MFS), drug/metabolite transporter (DMT) superfamily (i.e., small multidrug resistance (SMR) family), multidrug and toxic compound extrusion (MATE) family (i.e., multidrug/oligosaccharidyl-lipid/polysaccharide (MOP) flippase superfamily), and resistance-nodulation-division (RND) family [16]. Notably, the last family is prevalent in diderm rather than monoderm bacteria [20]. Recently, the proteobacterial antimicrobial compound efflux (PACE) family and the *p*-aminobenzoyl-glutamate transporter (AbgT) family have also been recognized as novel classes of AMR-secondary active transporters [21,22]. An inhibitor targeting these efflux pumps is a promising approach to restoring the activity of other antibiotics. Efflux pump inhibitors (EPIs) targeting secondary active transporters have been identified, such as pyridylpiperazine-based compounds targeting AcrAB-TolC [23], berberine (BBR) targeting MdfA [24], and samarium oxide nanoparticles, which target MFS coding genes [25]. TransportDB reported 516 active transporters from 47 classes within the *C. difficile* 630 genome. 141 transporters have been identified as secondary active transporters [26]. Schindler and Kaatz hypothesized that the genome of *C. difficile* 630 encoded 45 AMR-active transporters chromosomally. Most of them have been designated as secondary active transporters (13 MFS, 15 MATE, 2 DMT, and 1 RND); the remainder are ABC transporters [27]. We systematically analyzed ABC transporters in *C. difficile* 630 [19]; but the complete and systematic classification of secondary active transporters in *C. difficile* is still lacking.

In the present work, we systematically analyzed secondary active transporters of *C. difficile* 630 with emphasis on AMR association. To achieve this, we utilized sequence-based and structure-based identification and classification. Together with gene expression study of these transporters under antibiotic exposure using RT-qPCR and published transcriptome data, we identified novel AMR-secondary active transporters and revealed their evolutionary relationship. Using pangenome analysis, we classified AMR-secondary active transporter genes into core and accessory genes. Core genes are genes that are present in all analyzed genomes, while accessory genes are only identified in some of the genomes. Pangenome analysis allows us to better understand the evolution of these genes within the species. Certain AMR-secondary active transporters could potentially serve as targets for the development of EPIs that may enhance antibiotic activity against *C. difficile*. Our discoveries will be a basis for future works on the functional and evolutionary study of these transporters and pave the way for future drug development.

2. Results

2.1. The repertoire and classification of secondary active transporters of *C. difficile* 630

To establish a complete repertoire of secondary active transporters in the reference genome of *C. difficile* 630, we initially used protein sequence motif(s) for annotation (Fig. 1). We collectively identified consensus motifs for four (super)families known to be associated with antibiotic resistance, namely DMT (i.e., SMR), MATE (i.e., MOP), MFS, and RND, from the published data. We retrieved 12 MFS motifs, 30 DMT motifs, 4 MATE motifs, and 5 RND motifs (Suppl. Table 1). Identified motifs were less conserved and varied, rendering them inappropriate for manually identifying proteins in the reference genome of the *C. difficile* 630. Following that, we performed sequence alignment to identify the consensus motif by MEME suite server [28] using protein sequences from Pfam of each (super)family. Only a limited number of conserved motifs were identified across all (super)families, rendering them unsuitable for annotating secondary active transporters in the reference genome. Therefore, we redesigned the pipeline to construct a complete library of secondary active transporters. Our new pipeline involved initially extracting all membrane proteins, as we postulate that all transporters must be membrane proteins, followed by a sorting process to isolate secondary active transporters. In this study, we examined the entirety of the membrane proteins within the *C. difficile* 630 genome through deepTMHMM [29,30] and SOSUI [31]. These analyses showed that *C. difficile* 630 contains 996 and 1063 proteins harboring at least 1 transmembrane helix, according to deepTMHMM and SOSUI analyses, respectively. These amounts accounted for 26% and 27.8% of the total proteome of *C. difficile* 630, respectively. Finally, we identified all secondary active transporters in *C. difficile* 630 through annotations with Pfam [32] and InterPro [33] from the pool of membrane proteins (Suppl. Table 2). 141 proteins were identified as secondary active transporters and classified into 27 (super)families according to Transporter Classification Database, TCDB [34] (Table 1). Among the 27 (super)families identified, we focused on 5 AMR-(super)families including AbgT, DMT, MATE, MFS, and RND. We retrieved a total of 44 transporters, distributed as follows: 1 AbgT, 1 RND, 10 DMT, 14 MATE, and 18 MFS members (Table 1). From our inconclusive analysis using motif identification, we hypothesized that sequence similarity is probably insufficient to identify or classify secondary active transporters as the motifs are rather small and less conserved. Our speculation was confirmed by sequence-based phylogenetic analysis of AMR-secondary active transporters using the MAFF alignment [35] followed by PhyML tree construction [36,37] of 44 amino acid sequences of identified transporters.

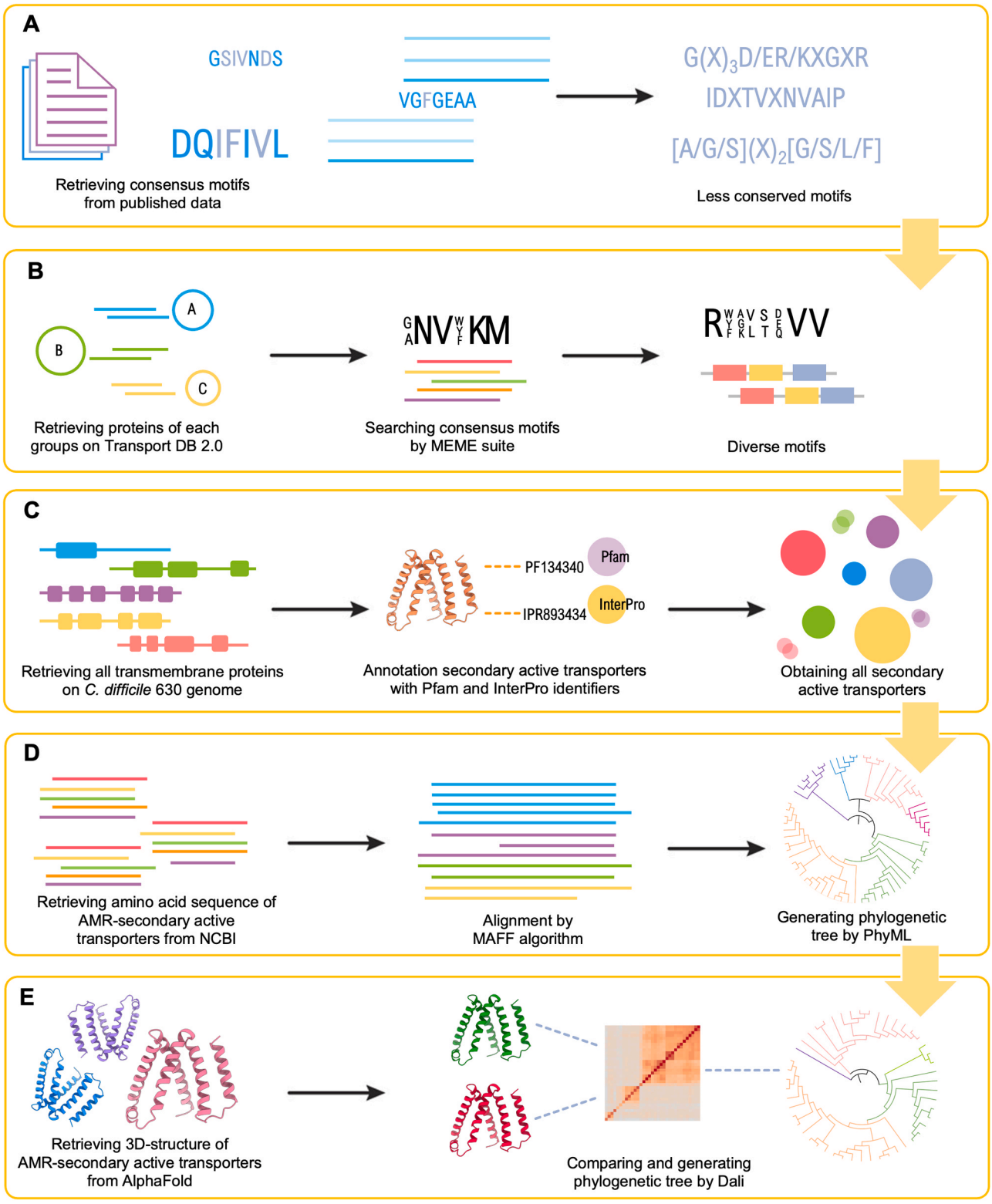

Fig. 1. Schematic of the construction of the secondary active transporter repertoire in the *C. difficile* 630 genome. Workflows represent (A) the motif-based analysis using published data, (B) the motif-based analysis using MEME suite, (C) the transmembrane domains-based analysis using deepTMHMM and SOSUI, (D) the sequence-based phylogenetic tree analysis, and (E) the structure-based phylogenetic tree analysis.

The sequence-based phylogenetic analysis suggested homogeneous grouping among MATE and DMT but there was incoherent grouping among AbgT, MFS, and RND (Suppl. Fig. 1). Except for MATE, this resulted in a paraphyletic assemblage of AbgT, DMT, MFS, and RND transporters due to the low similarity among members of each group. As Pfam and InterPro are mostly sequence-based annotations, we inferred that relying on sequence-based classification might not be adequate due to the overall sequence variability.

We then proposed that the proteins' 3D structures will better reflect their putative functions and may support their classification. Therefore,

Table 1
List of secondary active transporter (super)families retrieved from Pfam

(Super)Family	TC No.[a]	Count	Substrate and function
2-Keto-3-deoxygluconate transporter (KdgT)	2.A.10	2	2-Keto-3-deoxygluconate
Alanine or glycine: cation symporter (AGCS)	2.A.25	3	Na^+: Ala symporter
Amino acid efflux (AAE)	2.A.3	1	Asp: Ala antiporter
Amino acid-polyamine-organocation (APC)	2.A.3	6	Amino acid antiporter
Aromatic acid exporter (ArAE)	2.A.85	3	Fusaric acid
Arsenite-Antimonite (ArsB) efflux	2.A.45	1	As^{3+}
Auxin efflux carrier (AEC)	2.A.69	3	Indole 3- acetic acid
Branched chain amino acid: cation symporter (LIVCS)	2.A.26	3	Branched chain amino acid (BCAA)
C4-dicarboxylate uptake C (DcuC)	2.A.46	2	C4-dicarboxylate (C4DC) carrier
Divalent anion: sodium symporter (DASS)	2.A.47	1	Na^+: divalent anion/ sulphate symporter
Drug/metabolite transporter (DMT)	2.A.7	10[b]	Drug/metabolite/ quaternary ammonium
Glutamate: sodium symporter (ESS)	2.A.27	1	Na^+: Glu symporter
Major facilitator superfamily (MFS)	2.A.1	18[b]	H^+: peptides/drug symporter or antiporter
Membrane-bound acyl transferase (MBOAT)	2.A.50	2	Glycerol: H^+ symporter
Monovalent cation: proton antiporter-1 (CPA1)	2.A.36	3	K^+/Na^+: H^+ antiporter
Monovalent cation: proton antiporter-2 (CPA2)	2.A.37	1	K^+/Na^+: H^+ antiporter
Multidrug/oligosaccharidyl-lipid/ polysaccharide (MOP) (Included multidrug and toxic compound extrusion (MATE) family)	2.A.66	14[b]	Drug/multidrug: Na^+ and/or H^+ antiporter
Natural resistance-associated macrophage proteins (Nramp)	2.A.55	1	Mn^{2+}/Fe^{2+}
NhaC sodium: proton antiporter (NhaC)	2.A.35	4	Na^+:H^+ antiporter
Nucleobase: cation symporter-1 (NCS1)	2.A.39	1	Nucleotide: H^+/Na^+ symporter
Nucleobase: cation symporter-2 (NCS2)	2.A.40	8	Xan/Ura
p-Aminobenzoyl-glutamate transporter (AbgT)	2.A.68	1	*p*-Aminobenzoyl-glutamate
Resistance-nodulation-cell division (RND)	2.A.6	1	Multidrug/solvent
Riboflavin transporter (RFT)	2.A.85	3	Biotin/riboflavin/Typ
Solute: sodium symporter (SSS)	2.A.21	10	Na^+:H^+ symporter
Threonine/serine exporter (ThrE)	2.A.79	3	N/A
Unclassified	N/A	35	Vary

[a] TC No. is from the Transport Commission (TC) system [118].
[b] We identified potential novel transporters: MATE (CD630_14990), 2 DMT (CD630_19690 and CD630_35060), and 3 MFS (CD630_07020, CD630_00340, and CD630_22010), using the Dali server for 3D-structure comparison. Finally, we included a total of 15 MATE, 12 DMT, and 21 MFS transporters in our classification analysis.

we retrieved all transmembrane protein, identified by deepTMHMM and SOSUI, models from the AlphaFold database [38] and utilized Dali 3D-structure comparison [39] for structural clustering. A phylogenetic analysis of the Dali results demonstrated that transporters within each group consistently clustered together within the same branch (Fig. 2). The structure-based dendrogram depicted a robust clustering pattern, and the correspondence analysis of their pairwise distances indicated that each transporter group formed a cohesive cluster (Fig. 3A). The structural similarity matrix, which was constructed using Dali Z-scores for pairwise protein comparisons, consistently revealed that individuals within each group displayed notable structural homogeneity. Specifically, MATE and MFS have high structural similarity within the family, whereas DMT members exhibited only slight similarity among themselves (Fig. 3B). By using structure-based classification, we have unequivocally classified AMR-secondary active transporters into 5 (super) families and identified 1, 2, and 3 potentially novel MATE, DMT, and MFS transporters, respectively (Fig. 2). NCBI records CD630_14990 as a putative membrane protein, which is a novel putative MATE member. Putative DMT members, CD630_19680 and CD630_35060, are hypothetical proteins and putative membrane proteins, respectively. CD630_07020, CD630_00340, and CD630_22010, which have been designated as a putative membrane protein, putative xylose transporter, and transporter, respectively, are potentially novel MFS members. Altogether, a total of 147 secondary active transporters were compiled; 50 (34%) of which are AMR-secondary active transporters including 1 AbgT, 1 RND, 12 DMT, 15 MATE, and 21 MFS. The remaining 97 (66%) secondary active transporters may not be associated with AMR, and therefore are not of particular focus for this work.

To further explore the evolutionary relationships of secondary active transporters among *C. difficile*, 158 genome sequences were obtained from the NCBI database. Pangenome analysis revealed that secondary active transporters are equally classified as core and accessory genes; 49% of the genes encoding secondary active transporters in *C. difficile* 630 were classified as accessory genes, whilst the other 51% were designated as core genes. (Fig. 4). This distribution underscores the remarkable diversity and adaptability of these transporters within the *C. difficile* species. Focusing solely on the 5 (super)families associated with AMR, it's noteworthy that 67% of them are categorized as accessory genes, while 34% are considered core genes (Fig. 4).

2.2. Characteristics of AMR-secondary active transporters on C. difficile 630 genome

Secondary active transporters are of critical importance in various cellular processes, facilitating the entry of vital nutrients while expelling deleterious substances like biocides and antibiotics. Transporters of this nature play an essential function in cellular homeostasis maintenance, growth promotion, and reproduction facilitation [40,41]. To investigate the biological functions of AMR-secondary active transporters in response to biotic, abiotic stresses, and antibiotic exposure, we performed a thorough analysis of gene expression based on our RT-qPCR results and the datasets retrieved from previous transcriptome studies [42–45]. Stresses were grouped into antibiotics (RT-qPCR and microarray), abiotic stresses, and biotic stresses, as illustrated in Fig. 5.

We performed RT-qPCR to determine expression level during the treatments of eight antibiotics. We chose these antibiotics because they have been reported as substrates for efflux pumps [46] and/or treatments for CDI [7,8]. Several efflux pumps have been reported as multidrug efflux pumps [47]; therefore, different classes of antibiotics with different targets were included in our RT-qPCR. The eight antibiotics belong to 6 chemical classes including β-lactams (cloxacillin), glycopeptides (vancomycin), nitroimidazoles (metronidazole), lincosamides (lincomycin), macrolides (erythromycin and fidaxomicin), and fluoroquinolones (ciprofloxacin and levofloxacin). Cloxacillin and vancomycin inhibit peptidoglycan synthesis [48,49]. Metronidazole interacts with DNA causing the breakage of DNA strands [50]. Lincomycin and erythromycin bind to 23S rRNA of the 50S ribosome subunit, inhibiting protein synthesis [51]. Fidaxomicin targets RNA polymerase, which inhibits transcription [52]. Fluoroquinolones target type IV-topoisomerase and type II-topoisomerase (DNA gyrase) to form the quinolone-topoisomerase-DNA ternary complex, which arrests DNA replication [53,54]. Unlike the other six antibiotics, cloxacillin and ciprofloxacin are not effective against gram-positive bacteria. However, they are the empirical therapy for infectious diseases and were thus included in the gene expression study of AMR-secondary active transporters.

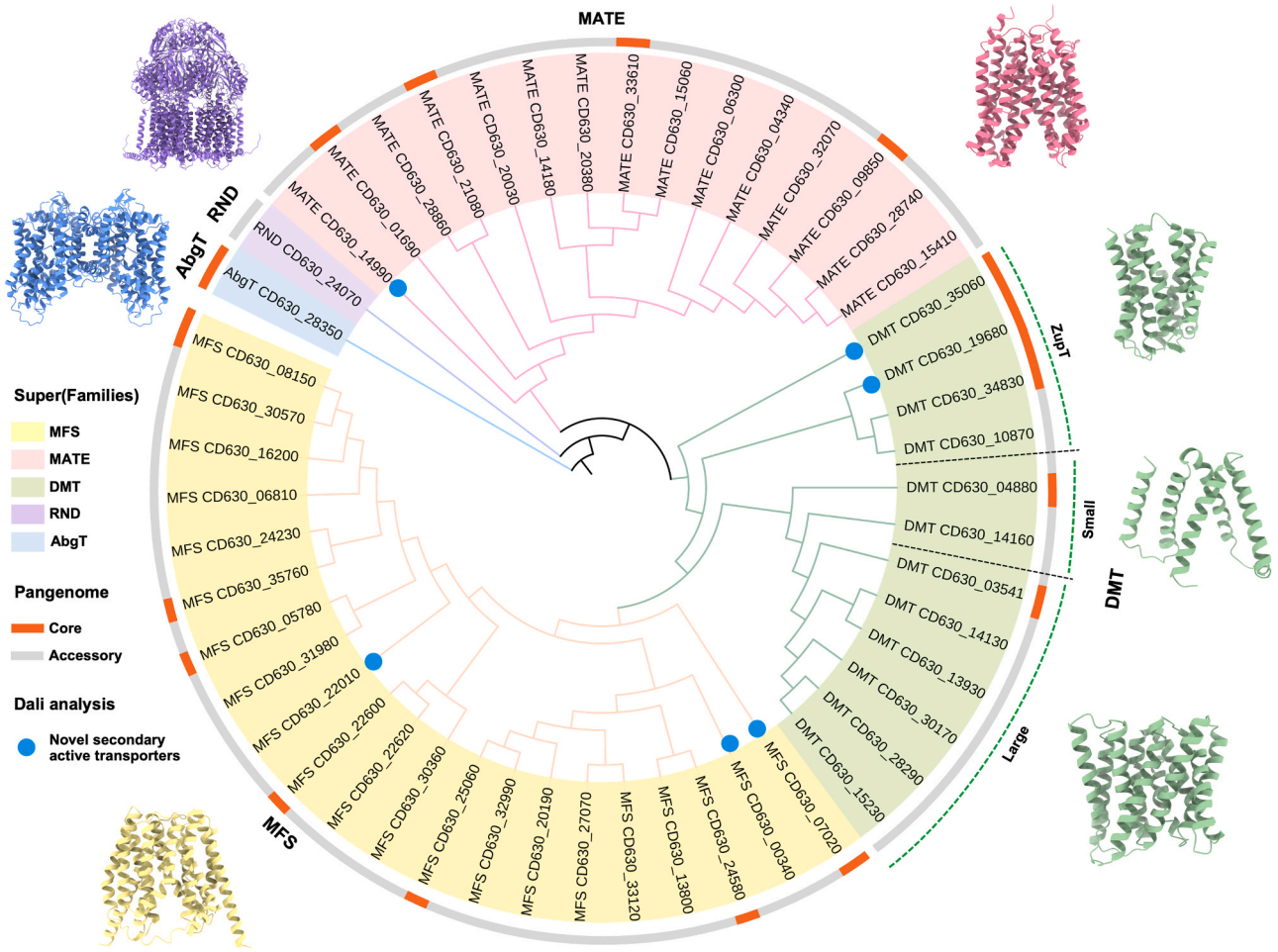

Fig. 2. Phylogenetic tree of 50 AMR-secondary active transporters on *C. difficile* 630 genome derived by protein structure similarity. The tree was constructed by average linkage clustering of the Z-scores from the Dali server. AMR-secondary active transporters are classified into 5 (super)families according to protein structure similarity. Blue dots at the tip indicate the novel, putative secondary active transporters identified by structural comparison. The outer circle illustrates core (orange) and accessory (gray) genes from pangenome analysis of 158 *C. difficile* genomes. Protein structures shown are representative for each (super)family and were from AlphaFold database: CD630_28350 (UniProt: Q183S2) for AbgT; CD630_24070 (UniProt Q181Y9) for RND; CD630_14180 (UniProt Q18BT5) for MATE; CD630_34830 (Uniprot Q180Y1) for ZupT; CD630_14160 (UniProt Q183R3) for small DMT; CD630_30170 (UniProt Q184K7) for large DMT; CD630_24230 (UniProt Q18BT7) for MFS.

Gene expression profiles revealed that all transporters from AMR-(super)families: MFS, MATE, DMT, RND, and AbgT, were prominently upregulated during antibiotic treatments, as well as biotic treatments rather than abiotic treatments (Fig. 5). The expression profile raised the assumption that transporters belonging to the five AMR-(super)families associate with antibiotic resistance and pathogenicity. Our RT-qPCR analysis supported that all genes from the five AMR-(super)families exhibited statistically significant changes in gene expression levels (Friedman's ANOVA, $p < 0.001$) when exposed to the eight antibiotics tested at their respective MICs (Fig. 5 and Suppl. Fig. 2). Fidaxomicin, metronidazole, levofloxacin, erythromycin, and lincomycin strongly induced the systematic upregulation of all AMR-super(families), whereby 94.6% of genes were upregulated by 50% (Fig. 5). Vancomycin induced the systematic upregulation of MATE, DMT, RND, and AbgT (96.6% of them were upregulated by 50%), while more than half (57.2%) of MFS genes were upregulated up to 50% (Fig. 5). Cloxacillin also induced the systematic upregulation of all five AMR-(super)families; however, it had a small effect on the expression of DMT (Fig. 5). The effect of antibiotics on AMR-secondary active transporter gene expression was evaluated by ranking the mean of induction fold change. Fidaxomicin was the strongest inducer (8.58-fold) followed by lincomycin (4.18-fold), erythromycin (2.54-fold), metronidazole (2.45-fold), levofloxacin (2.44-fold), vancomycin (2.28-fold), cloxacillin (2.04-fold), and ciprofloxacin (1.91-fold). As a result, we proposed that drugs active against gram-positive anaerobic bacteria can be stronger inducers than empirical antibiotics. In addition, drugs targeting RNA, DNA, and protein synthesis are stronger inducers for the upregulation of AMR-secondary active transporters than drugs targeting peptidoglycan synthesis. Most AMR-secondary active transporters showed limited response to abiotic stimuli (Fig. 5). However, biotic factors seemed to systematically upregulate the expression of AMR-secondary active transporter genes but not as high as antibiotics (Fig. 5). We proposed that AMR-secondary active transporter genes are more responsive to antibiotics than other factors, which indicates an association between these secondary active transporters and the cellular response to these antibiotics. The following sections will contextually elaborate on each (super)family in greater detail.

2.2.1. *Major facilitator superfamily (MFS)*

MFS is the largest group of AMR-secondary active transporters in the genome of *C. difficile* 630 comprising 21 proteins (Fig. 2). We identified 3 novel MFS proteins (CD630_07020, CD630_00340, and CD630_22010) through whole proteome structural clustering using Dali. According to the NCBI database, CD630_07020 was identified as a membrane protein, CD630_00340 was identified as a xylose transporter, and CD630_22010 was identified as a transporter [55]. As amino acid sequences of MFS are

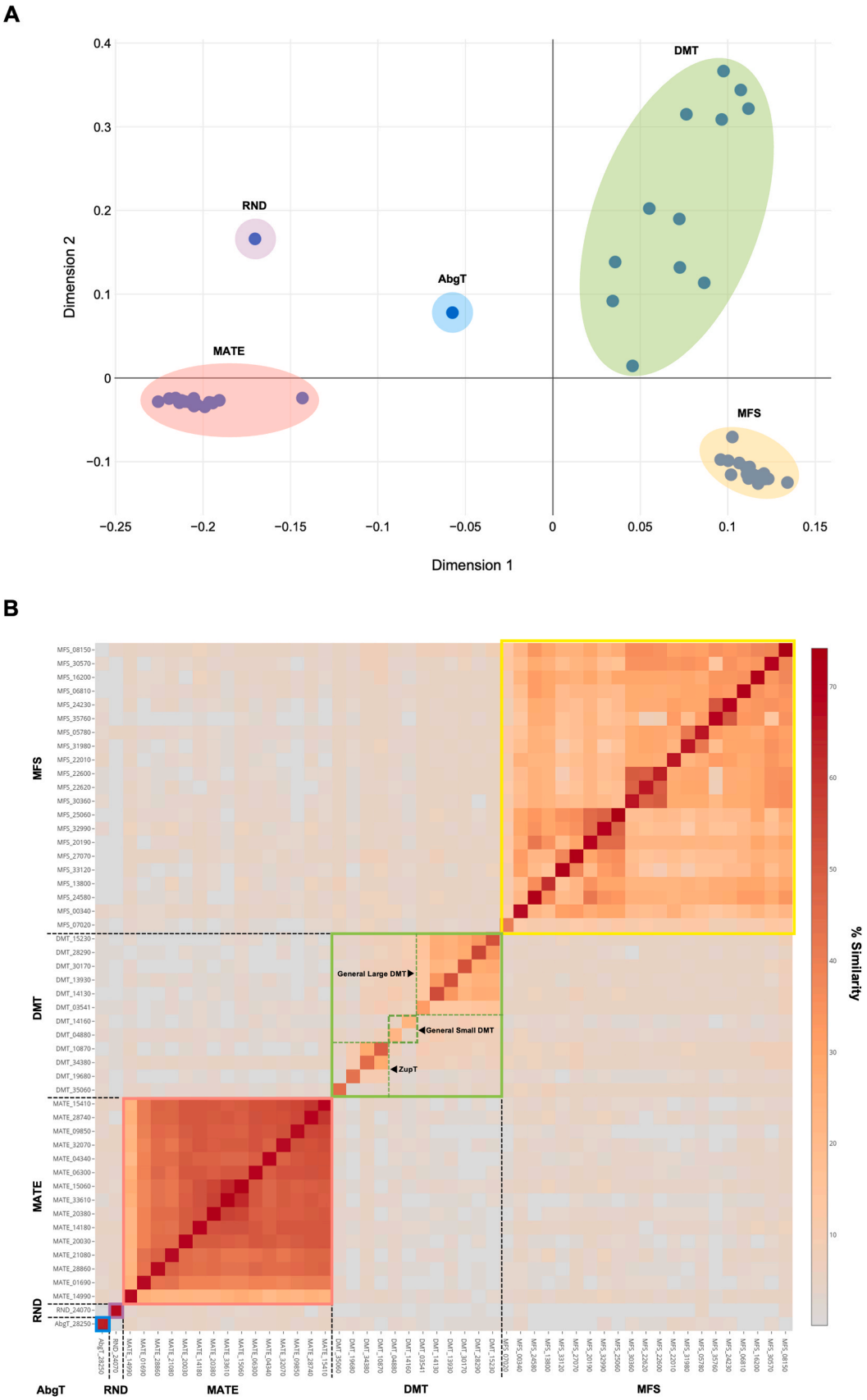

Fig. 3. Outputs from all-against-all protein structure comparison of 50 AMR-secondary active transporters of *C. difficile* 630 using Dali server. (A) The multidimensional correspondence analysis shows consistent clusters of AMR-secondary active transporters. (B) The similarity matrix generated by Dali Z-scores shows the homogeneity of each AMR-secondary active transporter (super)family. Yellow, green, pink, purple, and blue boxes indicate MFS, DMT, MATE, RND, and AbgT, respectively. The color indicates the similarity percentage between structures whereby, red is the highest similarity and gray is the lowest similarity.

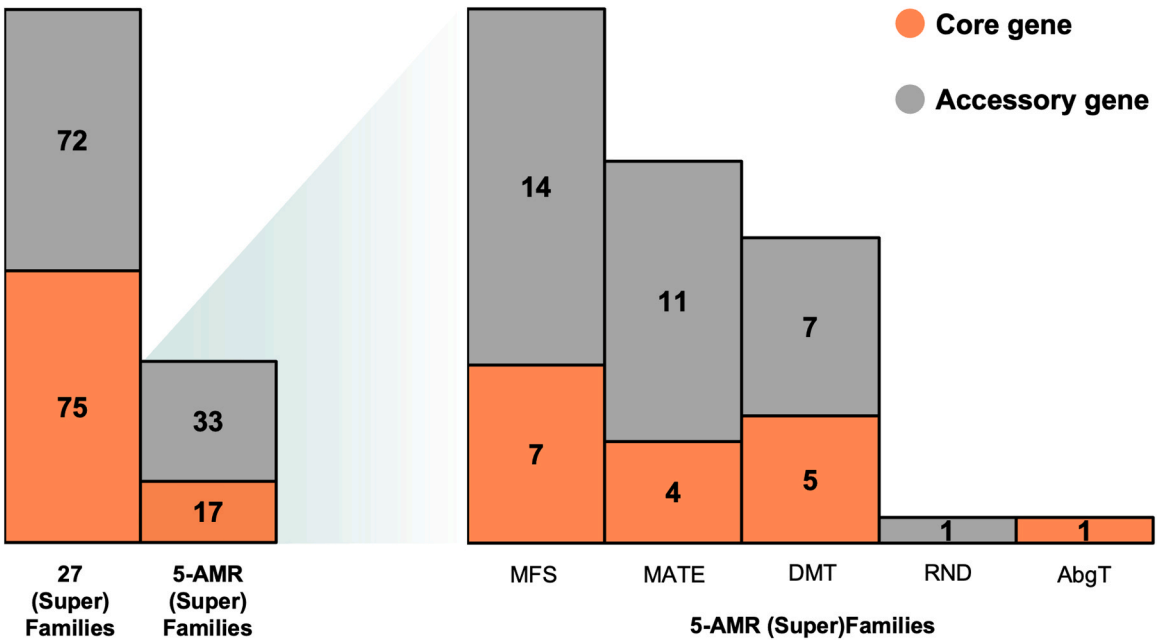

Fig. 4. Stacked columns of pangenome analysis on *C. difficile* 630 secondary active transporters. The charts illustrate core and accessory genes encoding secondary active transporters from 27 (super)families, 5 AMR-(super)families, and each AMR-(super)family. The numbers at the center of the plot indicate protein counts. Orange and gray indicate core and accessory genes, respectively.

diverse in both composition and length, a sequence-based phylogenetic tree grouped MFS with AbgT, DMT, and RND (Suppl. Fig. 1). A structure-based phylogenetic tree grouped all MFS separated from the rest of AMR-secondary active transporters as a monophyletic group (Fig. 2). MFS proteins exhibited a highly conserved structure (Fig. 3A–B). The RCSB PDB-pairwise structure alignment also showed a remarkable similarity score of 91–94% (Suppl. Fig. 3A). MFS has 8–14 transmembrane helices and most MFS have 12 transmembrane helices. Among the small MFS, CD630_07020, and CD630_00340 have 8 and 9 transmembrane helices, respectively. CD630_27070 and CD630_05780 have 10 transmembrane helices. CD630_16200 and CD630_30570 have 11 transmembrane helices. The largest MFS proteins, including CD630_13800, CD630_25060, and CD630_32990, have 14 transmembrane helices. CD630_31980 has been experimentally characterized as an ortholog of NorA from *Staphylococcus aureus*, and it was named as Cme facilitating erythromycin resistance [56]. Pangenome analysis showed that 66.7% of MFS were classified as accessory genes (Fig. 4). TransportDB proposed that MFS is a proton-driven transporter, serving as either proton:peptides/drug symporters or antiporters [26] suggesting diverse functions for MFS (Table 1). The substrate prediction was supported by the characterization of Cme [56].

Our RT-qPCR and microarray [42] reaffirmed the role of MFS in multidrug resistance (Fig. 5 and Suppl. Fig. 2). The MFS proteins responded largely to all 8 antibiotics tested. To disclose the ability and specificity of MFS transporters, which were induced by various antibiotics, the induction folds were sorted into quartiles. The genes that were sorted to the first quartile were considered the top 25% of the upregulated induction folds. *CD630_24230* was the top 25% of upregulated genes against 8 antibiotics, followed by *CD630_35760* with 7 drugs (except CIP), *CD630_33120* with 5 drugs (FDX, MTZ, LVX, LMC, CLO), *CD630_05780* with 5 drugs (FDX, MTZ, LVX, ERY, LMC), *CD630_25060* with 5 drugs (MTZ, LVX, LMC, VAN, CLO), *CD630_22600* with 4 drugs (CIP, LVX, LMC, CLO), *CD630_13800* with 3 drugs (FDX, CIP, ERY), *CD630_07020* with 2 drugs (ERY, VAN), *CD630_24580* with 2 drugs (CIP, CLO), *CD630_32990* with 2 drugs (FDX, MTZ), *CD630_08150* with 2 drugs (CIP, ERY), *CD630_00340* with VAN, *CD630_30360* with CIP, and *CD630_22010* with VAN (Suppl. Fig. 2). Notably, 38% of MFS were upregulated by 50% for all antibiotics, while most MFS were upregulated by 50% for at least 3 drugs (Suppl. Fig. 2). Therefore, we proposed that MFS transporters are broad-spectrum efflux pumps. Additionally, certain MFS transporters were involved in physiological homeostasis during abiotic stresses and in pathogenicity during spore germination and in vivo infection processes (Fig. 5). During abiotic stresses, most of the MFS genes had slight up or downregulation responses, inferring that abiotic stresses may not be their primary stimuli (Fig. 5). Antibiotics more strongly increased the expression of MFS genes (95% CI = 2.85–3.91) than the induction from spore germination and in vivo infection (95% CI = 1.96–2.16) as well as abiotic treatments (95% CI = 1–1.22) (Fig. 5). These suggest a predominant function for MFS proteins in responding to antibiotic challenges rather than pathogenicity during in vivo infection and spore germination and homeostasis during abiotic stresses. Interestingly, 3 novel identified MFS genes (*CD630_07020*, *CD630_00340*, and *CD630_22010*) were upregulated upon most antibiotic exposure (95% CI = 1,99–3.99, 1.10–2.89, and 1.10–1.80, respectively) except ciprofloxacin (Fig. 5 and Suppl. Fig. 2). Ciprofloxacin treatment resulted in down regulation of these genes by at least 50% (0.47, 0.34, and 0.28-fold, respectively). In addition, cloxacillin downregulated the level of *CD630_22010* by 83% (0.17-fold). These gene expression patterns suggest strong association between these genes and antibiotic resistance.

2.2.2. *Multidrug and toxin extrusion (MATE) family*

MATE is the second-largest secondary active transporter group within the *C. difficile* 630 genome. This family comprises 15 proteins and is closely related to DMT, as evidenced by phylogenetic analyses (Fig. 2). Based on our analysis, we successfully discovered one novel putative MATE member, CD630_14990, through structural clustering using Dali comparison, annotated as MurJ flippase [55]. MATE transporters have 10–14 transmembrane helices (TMHs). The smallest MATE is CD630_21080, comprising 10 TMHs. The largest MATE is CD630_14990, containing 14 TMHs. CD630_01690 and CD630_15140 possess 11 TMHs. The remaining MATE are designated as MepA, characterized as substrate-responsive regulatory proteins, and they possess either 11 or 12 TMHs. MepA-like proteins with 11 TMHs include CD630_33610, CD630_04340, and CD630_06300. The remaining MepA-like proteins with 12 TMHs are CD630_20030, CD630_14180, CD630_20230,

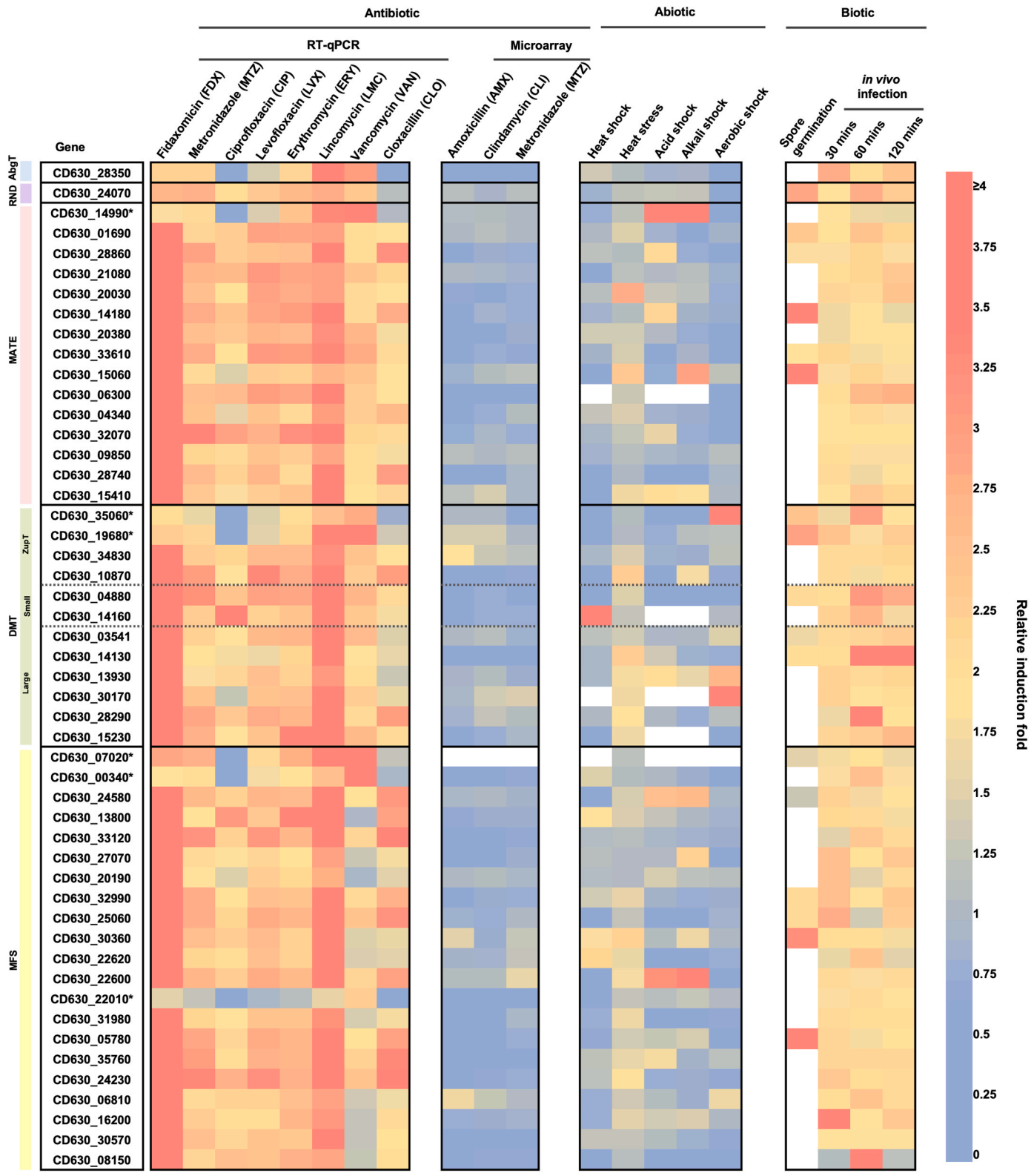

Fig. 5. Expression levels of genes encoding 5 (super)families of AMR-secondary active transporters during antibiotics, abiotic, and biotic treatment with induction fold scale. Colors indicate differential expression level, where red indicates up-regulation and blue indicates down-regulation. Treatment conditions are indicated on the top. Antibiotic treatments are separated into RT-qPCR, performed in this study, and microarray data published previously [42]. The abiotic treatments including heat stress, heat shock, acid, alkali, and aerobic condition were incorporated from published data [42,44] as well as spore germination [45] and in vivo infection [43]. Asterisks after the gene name indicate the novel putative secondary active transporters identified from protein structure clustering. White boxes indicate the absence of data.

CD630_15060, CD630_32070, CD630_09850, and CD630_28740. CD630_06300 is CdeA, as revealed via a BLAST result, which is the first MATE identified in *C. difficile* [57]. CdeA has been experimentally characterized as an ethidium bromide and acriflavine transporter, shown to mediate fluoroquinolone resistance when heterologously expressed in *E. coli* [57]. MATE proteins exhibited highly conserved structure and high similarity scores among their members (Fig. 3B and Suppl. Fig. 3B). MATE proteins also exhibited moderate conservation in their amino acid sequences. This family is classified into three sub-families: eukaryotic MATE (eMATE), NorM, and DNA damage-inducible protein F (DinF), based on their primary sequences. We subsequently classified 15 *C. difficile* 630 MATE proteins into sub-families based on amino acid sequence alignment using MAFF. Alignment showed all *C. difficile* 630 MATE belong to the DinF sub-family, as they share two distinct residues, D85 and D249, which are located within the N-terminal motifs NV(I)I(V)D and NII(V)LD, respectively (Suppl. Fig. 4). These are conserved signature residues within DinF members [58]. Pangenome analysis indicated that 26.7% of MATE are core genes (Fig. 4). TransportDB proposed that MATE function as multidrug transporters with Na^+ or H^+ or combines Na^+ with H^+ for an antiport mechanism in line with CdeA [57]. So, we hypothesized that all other MATE proteins may use a Na^+ and/or H^+-derived electrochemical gradient similar to CdeA and other MATE from other bacteria [59].

Our RT-qPCR results demonstrated statistically significant upregulation of genes encoding MATE in response to all antibiotics tested (Fig. 5 and Suppl. Fig. 2), which agreed with reported microarray studies (Fig. 5). To disclose the ability and specificity of MATE, the induction folds were ranked into quartiles. *CD630_14180* were in the top 25% of upregulated induction folds with 6 antibiotics (FDX, MTZ, CIP, ERY, LMC, CLO), followed by *CD630_28860* with 4 drugs (FDX, MTZ, LMC, CLO), *CD630_33610* with 4 drugs (MTZ, LVX, ERY, VAN), *CD630_32070* with 4 drugs (MTZ, CIP, ERY, LMC), *CD630_21080* with 3 drugs (CIP, LVX, ERY), *CD630_06300* with 2 drugs (CIP, LVX), *CD630_28740* with 2 drugs (FDX, CLO), *CD630_15410* with 2 drugs (FDX, LMC), *CD630_14990* with VAN, *CD630_01690* with LVX, *CD630_20380* with VAN, *CD630_15060* with VAN, *CD630_04340* with CLO (Suppl. Fig. 2). Eight (53%) MATE transporters were broad-spectrum efflux pumps as they were the top 25% of induction folds for at least 2 drugs. Notably, 4 (27%) MATE transporters may be narrow-spectrum efflux pumps as they were the top 25% of induction folds for vancomycin (*CD630_14990*, *CD630_01690*, and *CD630_20380*) and cloxacillin (*CD630_04340*). We speculated that these 4 MATE transporters may have substrate preference. 86.7% of MATE transporters were upregulated by 50% for eight antibiotics. Interestingly, 8 (53%) MATE transporters have a high expression (>8.39-fold increase) upon fidaxomicin exposure compared to the rest of the MATE members (Suppl. Fig. 2). Certain MATE proteins appear to participate in both abiotic and biotic responses (Fig. 5). However, we speculated that MATE contributes more toward antibiotic responses rather than abiotic and biotic conditions, as changes in gene expression are more pronounced during antibiotic stresses: the 95% CI of induction folds by antibiotics was 2.82–4.27; by abiotic treatments was 1.01–1.85; and by biotic conditions was 1.82–2.57 (Fig. 5 and Suppl. Fig. 2). Proposing that CD630_14990 may be the novel putative MATE transporter, we then analyzed the expression upon antibiotic treatments. Our RT-qPCR firmly supported that *CD630_14990* is associated with antibiotic resistance, since it was upregulated by 50% for most antibiotics (95% CI = 1.41–3.53) except ciprofloxacin and cloxacillin (Suppl. Fig. 2).

2.2.3. Drug/metabolite transporter (DMT) superfamily

There are 12 proteins classified as DMT within the genome of *C. difficile* 630 (Fig. 2), and two new DMT members have been identified in this study. Though DMT proteins were previously recognized as members of the SMR family, currently, the SMR family is considered a subfamily within the broader DMT superfamily [60]. Notably, DMT is the most heterogeneous cluster, exhibiting the lowest structural similarity compared to MFS and MATE (Fig. 3 and Suppl. Fig. 3C). Members of *C. difficile* 630 DMT have 4–10 TMHs as other prokaryotic DMT [61]. Variation of TMH contributes to the structural heterogeneity among the DMT [61]. Therefore, we divided the DMT superfamily into two groups, including ZupT and the DMT group based on intrinsic functions. The ZupT group comprises 4 proteins possessing 6–7 TMHs. They facilitate zinc uptake to regulate intracellular and extracellular zinc ion concentrations, contributing to zinc balance [62,63]. Within the ZupT group, CD630_10870 and CD630_34830 are canonical ZupT transporters [55]. CD630_19680 and CD630_35060 are novel putative ZupT, identified by structural clustering using Dali comparison. Currently, CD630_19680 and CD630_35060 are classified as a membrane protein and an uncharacterized hypothetical protein in the NCBI database, respectively. CD630_19680 and CD630_10870 have 6 TMHs, while CD630_34830 has 7 TMHs. Eight proteins in the DMT group have 4–10 TMHs; as a result, they were divided into two subgroups based on their number of TMHs: small DMT (4–5 TMHs) and large DMT (10 TMHs). Small DMT comprises 3 proteins including 4-TMH proteins (CD630_04880, CD630_14160) and 5-TMH protein (CD630_03541). Large DMT is characterized by 10 TMHs including CD630_14130, CD630_13930, CD630_30170, CD630_15230, CD630_35060, and CD630_28290. Small DMT facilitates multidrug, metabolite, and quaternary ammonium compound transport, while large DMT facilitates drug and metabolite transport (Suppl. Table 2).

Our RT-qPCR and published microarray [42] showed that all DMT were upregulated (95% CI = 2.61–3.51) upon antibiotic exposure. Most DMT responded to antibiotic exposure in our RT-qPCR gene expression assay (Fig. 5 and Suppl. Fig. 2). Transcriptome analyses [43–45] illustrated that DMT exhibits a lower response to abiotic conditions (95% CI = 0.85–2.68) but displays a heightened response during spore germination and in vivo infection (95% CI = 2.09–2.44) (Fig. 5). Their upregulation during spore germination and in vivo infection likely serves pathogenic functions related to metabolite transport, nutrient uptake, and possibly virulence factors, which are intrinsic functions of the DMT [61]. Our RT-qPCR suggested that ZupT transporters are less responsive to biotic treatments (95% CI = 1.98–2.37) than the DMT (95% CI = 2.10–2.52). This is also the case for antibiotic treatments where ZupT is slightly less upregulated (95% CI = 2.04–3.57) than the DMT (95% CI = 2.63–3.70). While ZupT showed limited response (95% CI = 0.47–1.79) to abiotic stresses, the DMT tended to respond more (95% CI = 0.81–3.39) to abiotic stresses. Notably, *CD630_10870* displayed a significantly higher response (>2-fold) to fidaxomicin compared to *CD630_34830* (Suppl. Fig. 2). This difference suggests a potential specialization or differential role for *CD630_10870* in the response to fidaxomicin. Moreover, RNA sequencing illustrated that *CD630_10870* was upregulated to 3.61-fold in the low iron condition, suggesting an important role in iron uptake and maintaining cellular iron concentration [64]. So, *CD630_10870* may play a crucial role in both antibiotic resistance as well as iron regulation. The DMT transporters showed an expression pattern akin to ZupT transporters, as they were more responsive to antibiotic treatments than abiotic or biotic treatments. However, the effects of antibiotics on the DMT were more pronounced than those on ZupT (Fig. 5). Small and large subgroups of the DMT showed the same pattern of gene expression; however, the induction folds of small DMT transporters were higher (95% CI = 2.54–4.13) than those of the large DMT (95% CI = 2.45–3.76) in antibiotic treatments.

Seven (58.3%) DMT transporters were upregulated by 50% for all antibiotics, supporting the broad-spectrum efflux pump hypothesis of DMT (Suppl. Fig. 2). To test this hypothesis, we sorted the induction folds by quartiles. *CD630_14160* and *CD630_15230* were in the top 25% of the induction folds against 6 drugs (FDX, MTZ, CIP, ERY, LVX, CLO for *CD630_14160* and MTZ, CIP, ERY, LVX, LMC, CLO for *CD630_15230*) followed by *CD630_34830* with 4 drugs (FDX, MTZ, CIP, CLO), *CD630_10870* with 4 drugs (CIP, LVX, ERY, CLO), *CD630_14130* with 4 drugs (MTZ, LVX, ERY, VAN), *CD630_19680* with 3 drugs (CIP, LVX,

ERY), *CD630_30170* with 3 drugs (CIP, LVX, ERY), *CD630_03541* with 3 drugs (CIP, LVX, VAN), *CD630_04880* with 2 drugs (LVX, ERY), *CD630_35060* with VAN, and *CD630_28290* with CLO. Therefore, we proposed that DMT transporters were broad-spectrum efflux pumps. Moreover, the novel putative DMT transporters were upregulated by 50% for most antibiotics (95% CI = 1.15–2.22 for *CD630_35060* and 1.42–3.47 for *CD630_19680*). These results supported that the novel putative DMT transporters are associated with antibiotic resistance as they were in the top 25% of induction increase for at least 1 antibiotic.

Interestingly, the response pattern to antibiotics, abiotics, and biotics observed across all DMT suggested that, under normal conditions, DMT transporters were involved in nutrient uptake, metabolite export, and pathogenicity. When *C. difficile* was challenged by antibiotics, a hypothesis emerged: DMT proteins may switch their role to act as (multi) drug efflux pumps, potentially contributing to the bacterium's resistance against antibiotic exposure [64].

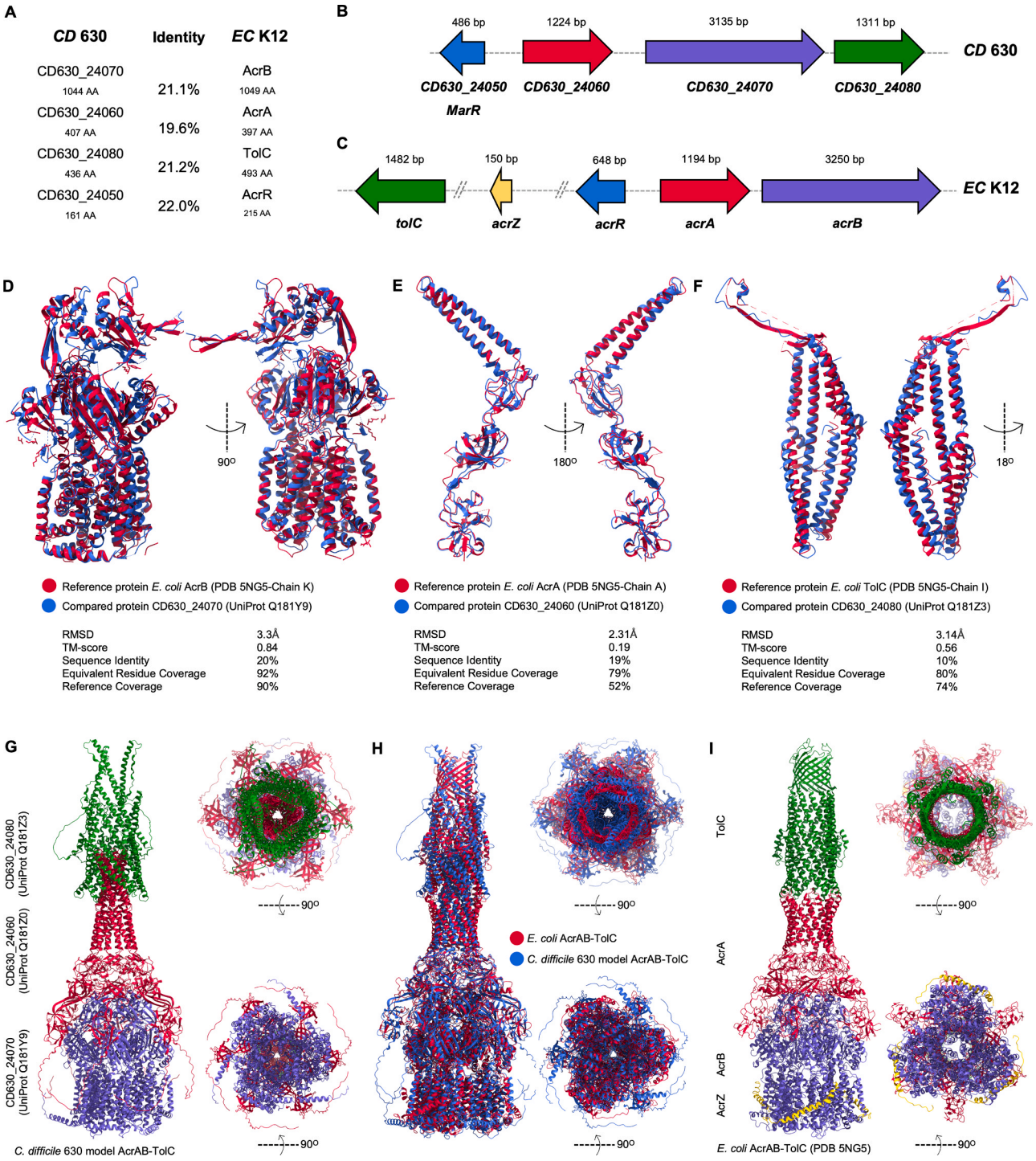

Fig. 6. Comparison between the AlphaFold model of *C. difficile* 630 RND and the cryo-EM structure of *E. coli* RND. (A) Amino acid similarity was analyzed by sequence alignment between subunits of *C. difficile* 630 RND and that of *E. coli* K12. The position and arrangement of genes encoding (B) *C. difficile* 630 RND and (C) *E. coli* K12 AcrAB-TolC: the schematics were generated based on the *E. coli* reference model [119]. (D–F) The comparative structural superimposition of each RND subunit shown with scores from RCSB PDB pairwise structure alignment. (G) RND model of *C. difficile* 630. (I) cryo-EM structure of *E. coli* AcrAB-TolC. (H) The comparative structural superimposition of the tripartite RND complex (*C. difficile* vs *E. coli*).

Pangenome analysis showed that 58.3% of DMT are accessory genes, while the remaining 41.7% are core genes (Fig. 4). 75% of ZupT are core genes that are highly responsive to abiotic and biotic conditions, compared to all DMT (Fig. 5); while 75% of the DMT are accessory genes that strongly responded to antibiotic treatments compared to all DMT (Fig. 5). Therefore, we proposed that the accessory genes of DMT are more associated with antibiotic resistance than abiotic and biotic responses. On the other hand, the core genes of DMT are associated with abiotic and biotic responses.

2.2.4. Resistance-nodulation-division (RND) family

Following the discovery of the RND member in the *C. difficile* genome, we examined the genomic landscape to identify the completeness of the RND complex in *C. difficile* using the Kyoto Encyclopedia of Genes and Genomes (KEGG) database in comparison with orthologs from the *Escherichia coli* AcrAB-TolC system [65]. The RND family is a well-known drug efflux protein family in gram-negative bacteria. The tripartite assembly comprises three functional units spanning their double membrane architecture, including an inner membrane protein (IMP), an outer membrane protein (OMP), and a periplasmic membrane fusion protein (MFP) that links the IMP and OMP [66]. Identifying the RND member within the genome of a gram-negative bacterium holds particular significance. We identified a gene from the RND family, namely *CD630_24070*. This locus encodes a 12-TMH protein, which is an ortholog of the IMP AcrB in *E. coli* (Fig. 6A–C). These results exceeded our expectations, since *C. difficile* is a monoderm, characterized by a single membrane layer in its architecture. However, prior research suggested the presence of a single RND protein within the *C. difficile* genome, as indicated by TransportDB. Collectively, these findings raise questions about the presence of the other components of the RND system within the genome of *C. difficile* 630.

We utilized *CD630_24070* as the reference locus to identify its potential complex partners within the vicinity. This identification was achieved by conducting orthologous comparisons with the AcrAB-TolC complex found in *E. coli* K12 using KEGG. Remarkably, we identified *CD630_24060* and *CD630_24080* as components of the RND system (Fig. 6A). The MFP encoding *CD630_24060* is an AcrA ortholog with 19.6% identity. The OMP encoding *CD630_24080* is a TolC ortholog with 21.2% identity. Therefore, it is evident that the genome of *C. difficile* 630 carries all the main functional components of the tripartite RND complex. Furthermore, we have identified the presence of a regulatory gene on the genome of *C. difficile* 630, known as *CD630_24050*, i.e., the MarR regulator. It is located upstream of the loci encoding the RND complex, akin to the role of the AcrR regulator in the RND complex of *E. coli* K12 (Fig. 6B–C). However, we were notably unable to identify the accessory AcrZ ortholog within the genome of *C. difficile* 630. We further compared the AlphaFold structures of the RND functional units of *C. difficile* 630 with the cryo-EM structure of the RND of *E. coli* using RCSB PDB pairwise structure alignment [67]. The pairwise structure showed that all components of *C. difficile* 630 displayed moderate to high coverage when aligned with their *E. coli* orthologs: CD630_24070 covered 90% of AcrB structure with 20% identity (Fig. 6D); CD630_24060 covered 52% of AcrA structure with 19% identity (Fig. 6E); and CD630_24080 covered 74% of TolC structure with 10% identity (Fig. 6F). Root-mean-square deviation (RMSD) suggested that the pairwise structure alignments between *C. difficile* RND and *E. coli* AcrAB-TolC were acceptable (2.31–3.30Å). The topological similarities between the *E. coli* AcrAB-TolC and *C. difficile* RND showed that CD630_24070 and CD630_24080 were similar to AcrB and TolC, respectively (TM-score >0.5; Figs. 6D and 6F). However, CD630_24060 was only slightly similar to AcrA (TM-score < 0.2; Fig. 6E). The RND complex of *C. difficile* 630 overall exhibits substantial structural conservation with that of *E. coli*.

Since we discovered *C. difficile* 630 harboring three units of the RND complex within its genome, the model should consider how they assemble as a whole complex. To this end, we used Chimera matchmaker through UCSF ChimeraX [68,69] to assemble the complete RND system. We also used the cryo-EM structure of the AcrAB-TolC of *E. coli* as a template structure [70], ensuring the same stoichiometry. The resulting complete RND model for *C. difficile* 630 exhibited remarkable similarity to the *E. coli* AcrAB-TolC complex (Fig. 6G–I). However, the structure of the MFP of *C. difficile* 630 RND appeared to be shorter than the AcrA, and there is a smaller cavity within the OMP of *C. difficile* 630 compared to that of *E. coli* (Fig. 6H). However, experimental structure elucidation is needed to confirm the hypothesis.

Pangenome analysis designated *CD630_24070* as an accessory gene (Fig. 4). TransportDB proposed that CD630_24070 may serve as a transporter for multiple drugs and solvents [26]. Our RT-qPCR analysis and published microarray data [42,43,45] verified its association with antibiotic resistance because our RT-qPCR showed significant upregulation during most antibiotic treatments (95% CI = 2.28–2.72; Suppl. Fig. 2), except ciprofloxacin and cloxacillin treatments. There is a possibility that *CD630_24070* may be involved in spore germination and in vivo infection according to transcriptomic data (95% CI = 2.03–2.85; Fig. 5). During abiotic conditions, *CD630_24070* was slightly changed (95% CI = 0.66–1.27) suggesting that it may be slightly involved in abiotic conditions. As CD630_24070 has two possible partners: CD630_24060 and CD630_24080. To determine whether CD630_24070 collaborates with its partners or functions independently, we also analyzed the gene expression of its partners and compared all using published microarray and transcriptional data [42–45]. During the amoxicillin, clindamycin, and metronidazole treatments, *CD630_24060* was marginally changed (95% CI = 1.06–1.26), whereas *CD630_24080* was slightly downregulated (95% CI = 0.74–0.94; Suppl. Fig. 5A). Abiotic factors induced more obvious changes in *CD630_24080* and *CD630_24060* expression (95% CI = 0.85–2.05 and 0.65–1.99, respectively) as well as spore germination (2.46 and 2.72-fold, respectively) and in vivo infections (95% CI = 2.11–2.45 and 1.84–2.56, respectively; Suppl. Fig. 5A). These expression patterns were observed in *CD630_24070* for antibiotic (95% CI = 0.94–1.13), abiotic (95% CI = 0.66–1.27), and biotic factors (95% CI = 2.03–2.85; Suppl. Fig. 5A). The results confirmed that the three genes are not pseudogenes, since they produced detectable mRNA and exhibited inducible expression. Therefore, we believe that CD630_24070 may collaborate with CD630_24060 and CD630_24080. Nevertheless, we proposed that CD630_24070 probably transports antibiotics and solvents and may function within *C. difficile* by natural system assembly but their assembly is still unknown and debated.

2.2.5. p-aminobenzoyl-glutamate (AbgT) family

CD630_28350 is the sole AbgT on the genome of *C. difficile* 630. AbgT functions as a homodimer [71]. CD630_28350 has 12 TMHs. TransportDB proposed that CD630_28350 was the importer of *p*-aminobenzoyl-glutamate, i.e., PABA-Glu (Table 1), corroborating with previous studies that proposed its role in the import of PABA-Glu for folate production and involvement in sulfonamide efflux [71]. The AlphaFold structure of CD630_28350 was highly conserved to the AbgT prototype, i.e., MtrF of *Neisseria gonorrhoeae* and YdaH of *Alcanivorax borkumensis* (Suppl. Fig. 6). The RMSD suggested that the pairwise structure alignments between CD630_28350 and MtrF, and between CD630_28350 and YdaH were acceptable (1.52 and 1.84Å, respectively). The topological similarities between CD630_28350 and its orthologs showed that CD630_28350 was highly similar to MtrF and YdaH, respectively (TM-score = 0.93 and 0.92, respectively; Suppl. Fig. 6).

Pangenome analysis indicated that *CD630_28350* is a core gene, consistent with its essential role in folate biosynthesis [72]. Previous transcriptomic analyses [42] showed the substantial downregulation of *CD630_28350* in response to amoxicillin, clindamycin, and metronidazole treatments (95% CI = 0.32–0.52; Fig. 5). Our RT-qPCR showed that *CD630_28350* was downregulated in response to ciprofloxacin (0.39-fold) and cloxacillin (0.62-fold). On the other hand, the

CD630_28350 was upregulated by 50% in response to fidaxomicin, metronidazole, levofloxacin, erythromycin, lincomycin, and vancomycin (95% CI = 1.88–2.88; Fig. 5 and Suppl. Fig. 2). These results suggested that CD630_28350 was associated with antibiotic resistance for several antibiotics. Moreover, transcriptome analysis [43] showed that *CD630_28350* was upregulated by 50% during in vivo infections (95% CI = 2.02–2.22; Fig. 5). This pattern of upregulation during infection supports its primary role as an importer of essential metabolites [21,73,74]. The response of *CD630_28350* to abiotic conditions [42,44] appeared to be limited (95% CI = 0.75–1.18; Fig. 5). Therefore, we hypothesized that AbgT in *C. difficile* 630 primarily functions as an importer of folate precursors and has an adaptive role in antibiotic resistance. It is limited to general physiological maintenance. Therefore, we proposed that AbgT belonging to *C. difficile* is strongly involved in antibiotic resistance and the import of folate precursors.

Considering these findings and the predominant gene response to antibiotic treatments, we hypothesized that secondary active transporters are strongly associated with antibiotic resistance in *C. difficile*. However, it is possible that these transporters may have additional roles in physiological maintenance processes as well.

3. Discussion

Transporters serve a crucial function in cellular homeostasis and the survival of cells by importing or exporting various substrates. Some transporters can export toxic substances including antibiotics leading to the AMR phenotype. *C. difficile* can employ several mechanisms for drug resistance, with the active transport of drugs out of the cell being one such mechanism [75–77]. Building upon our recent exploration of the complete collection of ABC transporters in *C. difficile* 630 [19], this study aims to systematically assemble the entire repertoire of secondary active transporters in the genome of *C. difficile* 630. Our goal is to examine the contribution of AMR-secondary active transporters to antibiotic resistance. This research will establish a foundation for further studies in drug resistance and drug discovery.

Within the genome of *C. difficile* 630, 28% of proteins are membrane proteins (1063 membrane proteins/3828 whole proteome). This aligns with previous reports that 20–30% of the bacterial proteome is made up of membrane proteins [78,79]. Among these, 226 are ABC transporters [19]; 147 are secondary active transporters; and the rest are other membrane proteins (Table 1). We classified 50 secondary active transporters as AMR-secondary active transporters belonging to 5 (super) families: AbgT, DMT, MATE, MFS, and RND. While there are 6 well-known prokaryotic AMR-(super)families, we could not identify any proteins belonging to the PACE family within the genome of *C. difficile* 630. It is noteworthy that this does not preclude the existence of PACE protein(s) in *C. difficile*. Based on our whole (membrane) proteome structural clustering, using Dali comparison, we identified 6 potential novel secondary active transporters in the genome of *C. difficile* 630: 1 MATE, 2 DMT, and 3 MFS. Our clustering of AMR-secondary active transporters was achieved through structure-based phylogenetic analysis, which successfully grouped 50 AMR-secondary active transporters into 5 main groups, providing a robust understanding of their evolution and functions. Our repertoire comprises 50 AMR-secondary active transporters, more than the curation by Schindler and Kaatz at 31 [27]. The rest of the secondary active transporters may serve innate biological functions including signal transduction, protein secretion, antigen presentation, bacterial pathogenesis, sporulation, and nutrient uptake [80,81], rather than conferring antibiotic resistance.

Initially, we utilized a conventional sequence-based phylogenetic analysis to classify AMR-secondary active transporters, but surprisingly failed to group them accordingly (Suppl. Fig. 1). We speculated that lacking a highly conserved sequence in each (super)family was the cause of the perplexed clustering (Suppl. Table 1). On the other hand, this posited that these (super)families are somewhat related. We then used AlphaFold structures for clustering AMR-secondary active transporters based on structural similarity. The results gracefully classified the transporters into 5 homogeneous groups, namely AbgT, DMT, MATE, MFS, and RND (Fig. 2). Our structure-based phylogenetic analysis supported the hypothesis that the amino acid sequence alone is insufficient to uncover the evolutionary relationship among AMR-secondary active transporters due to the low conservation of their consensus motifs. The protein structure is normally more conserved than the primary sequence to retain the conserved folds and functions [82]. Furthermore, structural clustering of the whole (membrane) proteome allowed us to identify 6 unannotated AMR-secondary active transporters, however, further experiments are required to verify the function of these proteins as AMR-secondary active transporters. The benefit of using structural homology to annotate or classify proteins has been evident in the recent adoption of this strategy by the Pfam database [32]. The advent of machine learning protein prediction software opens vast opportunities for protein structure-related research as the accuracy of the models has seen a leap in improvement compared to most conventional methods [83]. Recently, structure-based classification has been effectively revealing the evolutionary relationships among proteins, facilitating their classification and providing trustworthy annotations for novel proteins and their putative biological roles using AlphaFold structures [84,85]. Hence, our structure-based clustering analysis has the potential to shed light on the evolution of AMR-secondary active transporters in the genome of *C. difficile* 630. Furthermore, protein structure pairwise analysis using Dali is a powerful tool to perform phylogenetic and evolutionary analyses [86–88].

We hypothesized that the expression of genes encoding AMR-secondary active transporters should be induced during antibiotic exposures. RT-qPCR profiles revealed that all test antibiotics promoted increased transcription of AMR-secondary active transporter genes, affirming their roles in drug resistance response. Our findings also agreed with previous transcriptome data [42–45]. Our RT-qPCR showed that all genes encoding AMR-secondary active transporters were strongly upregulated upon exposure to metronidazole. However, the microarray from Emerson and colleagues [42] showed that only 11 AMR-secondary active transporters genes were slightly upregulated (Fig. 5). This discrepancy in expression level may be caused by different concentrations of antibiotics and incubation time. We incubated *C. difficile* 630 with the MIC (0.25 $\mu g \cdot mL^{-1}$) of metronidazole for a short period, while they incubated with a lower concentration (0.15 $\mu g \cdot mL^{-1}$) for longer [42].

Furthermore, we explored how genes encoding AMR-secondary active transporters respond to other stresses including biotic and abiotic stresses through published transcriptome data [42,43,45]. Some genes exhibited mild responses to abiotic stresses but displayed strong expression during spore germination and in vivo infection. These suggested that AMR-secondary active transporters of *C. difficile* possess multifunctionality, not only in pathogenicity and physiological roles, but also in antibiotic resistance. Interestingly, *C. difficile* showed the highest gene upregulation during fidaxomicin treatment, where all genes were upregulated. We believed that fidaxomicin increased the transcription of genes encoding AMR-secondary active transporters through regulation at the transcriptional level [16]. Moreover, it is thought to be the influence of efflux regulation due to fidaxomicin targeting RNA synthesis, causing rapid responses, since antibiotic-triggered RNA-mediated regulation is common in human pathogens [89].

Most AMR-secondary active transporters exhibit broad specificity for substrate utilization, allowing them to recognize a wide range of molecules, including drugs, metabolites, and dyes. Nevertheless, some transporters demonstrate narrow specificity [90,91]. The substrate specificity of AMR-secondary active transporters typically relies on the composition of amino acid residues located within the drug-binding cavity [92]. Substrate prediction reveals that AMR-secondary active transporters likely interact with multiple substrates, emphasizing their role as preferentially broad substrate efflux pumps. Furthermore, gene expression profiles provide support for the broad substrate hypothesis,

as almost all AMR-secondary active transporters exhibit upregulation when exposed to various antibiotics with different chemical classes. This observation suggests that a substantial portion of secondary active transporters respond to multiple substrates.

Here, we provide strong evidence that supports the role of well-known AMR-secondary active transporter (super)families, MFS, MATE, DMT, RND, and AbgT, in mediating multidrug efflux (Fig. 5). Both MFS and MATE showed highly conserved structure within the group (Suppl. Fig. 4). This inferred that they may share the same functions within the group. However, DMT showed structural diversity indicating lower structural similarity (Fig. 3 and Suppl. Fig. 3C). Therefore, it was split into 2 subgroups based on their putative functions and number of TMH: ZupT and the DMT. The DMT subgroup can be further classified into 2 subgroups: small and large DMT. Surprisingly, 3 genes encoding the RND complex (*CD630_24060*, *CD630_24070*, and *CD630_24080*) were identified and they are potentially functional genes, not pseudogenes since their expressions could be affected by certain stimuli.

RND is a well-known AMR-secondary active transporter in gram-negative bacteria [93,94]. Indeed, the RND represented a complex group within the AMR-secondary active transporter system. The SecDF family, a sub-family belonging to RND, was found not only in gram-negative bacteria, but also in gram-positive bacteria and archaea [95]. The SecDF family is a non-essential component of the type II secretion system (TIISS) protein secretory complex, which works via a coupling of substrate translocation and the proton motive force [96]. However, it also works in a partially ATP-dependent manner, which complicates its functionality. Therefore, we hypothesized that the RND of *C. difficile* 630 may belong to SecDF members, deriving the appearance and biological role of SecDF in *C. difficile*. Our hypothesis was supported by the SecD and SecF motifs in the amino acid sequence of CD630_24070. These motifs provide a proton electrochemical gradient [95]. Additionally, structural phylogenetic analysis (Suppl. Fig. 5B) and transmembrane domain comparison (Suppl. Fig. 5C) showed CD630_24070 was closely related to ABC transporters of *C. difficile* 630. These demonstrate the structural similarity between CD630_24070 and ABC transporters and explain the partial ATP-dependence of CD630_24070. This reflects, via structural constituents, an evolutionary relationship between ABC transporters and RND in *C. difficile*. The sister ABC proteins, CD630_03130, CD630_35840, CD630_04830, and CD630_19540, were of unknown family [19]. This may support the evolutionary bridge between ABC transporters and RND. However, these could at least partially be explained by conserving structural parts in both primary and secondary active transporters in *C. difficile* 630. The existence of RND in the genome of *C. difficile* 630 is thought to be a remnant from evolutionary divergence between monoderm and diderm bacteria. Gupta proposed that monoderm evolved from a common ancestor with diderm [97]. The common ancestor had 2 membrane layers to conquer environmental antimicrobial compounds and monoderm lost their outer membrane (OM) during evolution [98]. Fermicutes, which are mostly monoderm, have two diderm classes, namely Negativicutes and Halanaerobiales [98]. These Firmicutes are positioned as sister groups to Clostridiales. This observation suggests that the common ancestor of Firmicutes possessed genes encoding the OM; however, these OM genes have been lost during evolution in Clostridiales and other classes of Firmicutes including Thermoanaerobacterales, Bacillales, Lactobacillales, and Natranaerobiales [99,100]. We proposed that the retention of genes encoding RND in the genome of *C. difficile* 630 may be an evolutionary footprint of Firmicutes. It is conceivable that the far ancestors of Clostridia carried genes encoding the RND due to the presence of two membrane layers. Then, the closest Clostridia ancestor lost its OM genes during evolution, but the genes encoding RND were still carried on in the genome of some *C. difficile*, with *CD630_24070* as an accessory gene (Fig. 4). Lopez and colleagues also found 3 components of RND in the genome of *C. difficile* 630, constituting an operon. Their experimental validation, indicating *C. difficile* 630 RND contributes to toxic metabolites efflux and sub-cellular fractionation, suggested that CD630_24080, a TolC ortholog, was associated with surface-layer proteins (SLPs) and cell wall proteins [101]. Hence, the analyses conducted by Lopez and colleagues corroborated our findings regarding the presence and response of the RND on the genome of *C. difficile* 630. Their results suggested that these three genes are not pseudogenes, given their location within the regulatory region of the same operon. In the realm of evolutionary biology, it is imperative to examine the relationship of the RND system between *C. difficile* and other Firmicutes in comparison to gram-negative bacteria. This inquiry seeks to provide insights into why gram-positive bacteria, particularly *C. difficile*, bear three distinct components of the RND efflux pump, a feature that appears to be distinctive within the realm of gram-negative bacteria. Furthermore, structural elucidation of the RND system will provide solid proof of the arrangement and function of RND of *C. difficile* 630.

More than half of the AMR-secondary active transporters in the *C. difficile* 630 genome are accessory genes, according to pangenome analysis (Fig. 4), which supports our belief that these genes mediate antibiotic resistance rather than having physiological roles. According to our hypothesis, they should be found in all *C. difficile* strains if they are meant to be involved in essential physiological processes. Alternatively, it is conceivable that these genes may serve a redundant function with distinct variants. Consequently, it may not be imperative to carry a multitude of secondary active transporter genes within their genomes. In scenarios where certain strains lack specific genes, alternative gene variants could potentially fulfill the functions. However, the presence of these genes in the context of antibiotic resistance suggests that they may have been acquired from other bacterial donors. In practice, genes encoding secondary active transporters can have two origins: either they are part of the native genome, or they are obtained from mobile genetic elements such as transposons or donor plasmids before being incorporated into the genome [102]. The acquisition and insertion of resistance genes from external sources can make a substantial contribution to the evolution of antibiotic resistance in *C. difficile* strains [103–105]. Therefore, we suggested that this scenario could be happening within the genome of *C. difficile*, resulting in an abundance of accessory active transporter genes. Moreover, abundant accessory genes on the genome of *C. difficile* may be caused and maintained by selection during evolution [106]. Alternatively, we hypothesize that the gene duplication occurred during the evolution of *C. difficile* 630, leading to an extensive presence of accessory AMR-secondary active transporter genes in this strain. Genes involved in drug resistance have the potential to be duplicated during evolution. *hflX* genes and some heat shock proteins involved in drug resistance are reported to be duplicated in Firmicutes bacteria [107]. Moreover, RND genes have been proven to be duplicated in several bacteria, making them carry more than one copy in their genomes [108,109]. Moreover, a hundred gene duplications occurred in Firmicutes genomes during evolution, and those duplications involved the antibiotic resistance phenotype [110]. Thus, we proposed that the diversity of AMR-secondary active transporters, potentially serving similar functions, may be attributed to multiple instances of gene duplication. Notably, we believed that accessory AMR-secondary active transporter genes were possibly linked to virulence, antimicrobial resistance, or other environmental adaptations. However, core genes may also be involved in the pathogenicity of *C. difficile*. Pangenome analysis in *Streptococcus pneumoniae* illustrated that genes involving pathogenicity are core genes [111] and accessory genes of *Pseudomonas aeruginosa* are directly associated with pathogenicity [112]. These supported our hypothesis that both core and accessory genes of *C. difficile* are involved in pathogenicity and accessory genes may intend to involve AMR.

In a previous study, we proposed that *C. difficile* 630 harbors a total of 93 AMR genes [19]. Incorporating our analysis, we have identified that secondary active transporters make up 46% of the total AMR genes within the genome of *C. difficile* 630. Specifically, among the identified AMR genes, AMR-ABC genes account for 16% of the genome of

C. difficile 630 [19]. The prevalence of AMR-secondary active transporter genes in the *C. difficile* 630 genome is three times higher than that of AMR-ABC genes. Furthermore, within the genome of *C. difficile* 630, AMR-secondary active transporter genes makeup approximately 30.5% of the total secondary active transporter genes, whereas AMR-ABC genes constitute about 6.5% of the total ABC genes in the genome [19]. As such, the efflux of antibiotics exhibited by *C. difficile* 630 is mediated by secondary active transporters and ABC transporters. These analyses supported the hypothesis that *C. difficile* 630 uses active transport proteins as one of its main resistance mechanisms, which was supported by the diversity and prevalence of AMR-active transporter genes on the *C. difficile* 630 genome.

4. Conclusion

C. difficile employs several primary and secondary active transporters for homeostasis, pathogenicity, and antibiotic resistance mediation. We collected a total of 147 secondary active transporters belonging to 27 (super)families in the genome of *C. difficile* 630, 34% of which are AMR-secondary active transporters from the AbgT, DMT, MATE, MFS, and RND (super)families. We also identified 6 novel putative AMR-secondary active transporters through structure clustering that had not been previously annotated. Our findings highlight that protein structure, made possible by a machine learning protein prediction algorithm, can reveal more about AMR-secondary active transporter evolution than sequence similarities. We believed that the retention of genes encoding tripartite RND on the genome of *C. difficile* 630 might be an evolutionary footprint of Firmicutes, which shares a common ancestor with gram-negative bacteria. Gene expression profiles confirmed that AMR-secondary active transporters respond to antibiotics more than other stresses. We proposed that AMR-secondary active transporters can recognize various substrates due to their responses to broad substrates and antibiotics. We encourage that AMR-secondary active transporters should be extensively characterized as only a handful of AMR-secondary active transporters of *C. difficile* have been studied. Deeper understanding of these transporters could potentially lead to new therapeutics through efflux pump inhibitor discovery.

5. Materials and methods

5.1. Construction of secondary active transporter collection in C. difficile

The computational identification of a complete secondary active transporter system in *C. difficile* 630 was primarily based on Pfam [32] and InterPro [33], which were classified using multiple sequence alignments and hidden Markov models (HMMs) [29]. The whole genome of *C. difficile* 630 was used for retrieving all secondary transporter protein families from TransportDB [26] and codes of protein names were obtained. The protein names were annotated to Pfam [32] and then, mapped to InterPro [33] using the protein code.

To identify potentially missed AMR-secondary active transporters due to reduced amino acid sequence conservation, we sought to classify proteins according to their 3D structures using AlphaFold predicted structures. We obtained all membrane protein structures (based on TMHMM and SOSUI analyses) of *C. difficile* 630 from the AlphaFold database and ran an all-to-all pairwise comparison to generate a distance matrix using Dali software [39]. Overall AlphaFold model quality was favorable. Most model (~80%) have the median of pLDDT >90. Most membrane protein model have ~80% of residues with pLDDT >80 (Suppl. fig. 7). Any proteins with no clear annotation (or hypothetical) that fall into the same cluster with known groups of AMR-secondary active transporters were considered potentially novel.

5.2. Phylogenetic constructions

By gene annotation, we were able to construct a list of all potential secondary active transporters found in the *C. difficile* 630 reference genome. To categorize AMR-secondary active transporters, a phylogenetic analysis based on amino acid sequence similarity was built. Sequence similarity was elucidated by comparing the amino acid sequences using MAFFT multiple sequence alignment with the L-INS-i module [35]. Then the phylogenetic tree was analyzed based on mL inferences through PhyML version 3.0 [36]. Robustness of the tree topologies was defined as previously described by Martí -Solans, where it was assessed based on an automatic model using the Akaike Information Criterion (AIC) and inferred using the fast likelihood-based methods through aLRT Chi2-based branch support approach [37,113,114]. For phylogenetic analysis of AMR-secondary active transporter based on structure comparison, Z-scores from all-against-all Dali comparison were used to generate distance similarity matric and performed PhyML as per sequence-based analysis.

5.3. Identification of core and accessory genes

To identify core and accessory secondary active transporters in *C. difficile*, Bacterial Pan Genome Analysis tool (BPGA) software was used [115]. All available complete RefSeq *C. difficile* genomes (in the form of protein FASTA format files) totaling 158 (as of October 2023) were retrieved from the NCBI database and used as inputs for BPGA using default parameters. The USEARCH algorithm was used with a sequence similarity cut-off of 0.7. We employed the BPGA default USEARCH algorithm as it was shown to generate almost identical results to other algorithms, but faster than others. Sequence similarity cut-off of 0.7 was used, instead of the BPGA default of 0.5; because we are comparing genomes of the same species and, therefore, expecting them to have higher similarity of the same gene. Core and accessory gene IDs were called from the *C. difficile* 630 genome.

5.4. Transcriptomic profiles of secondary active transporter genes in C. difficile

Transcriptomic profiles of *C. difficile* 630 were obtained from numerous sources, as previously described, to provide a broad overview of the transcription dynamics of genes expressing secondary active transporters in *C. difficile* under stress conditions [19]. The stress conditions were divided into three groups: antibiotics treatment [42], physical stresses (including heat stress, heat shock, acid, alkali, aerobic condition [42,44]), spore germination [45], and in vivo infection [43]. All differential induction fold differences of AMR-secondary active transporter genes were presented by heatmap to enable comparisons between all treatments.

5.5. Gene expression analysis

We initially determined the minimal inhibitory concentration (MIC), following the Clinical and Laboratory Standards Institute (CLSI) standard (M11–A8) with certain modifications, to evaluate gene expression during antibiotic treatments (Suppl. Materials and Methods). Gene expression was studied by incubating mid-log phase *C. difficile* 630 with MIC of each antibiotic for 1 h. DMSO was used as a negative control. Total RNA was extracted using the Direct-zol RNA Miniprep kit (Zymo Research) according to the manufacturer's instructions. Total RNA was used to generate a cDNA library using iScript Reverse Transcription Supermix for RT-qPCR (Bio-Rad) according to the manufacturer's instructions. The qPCR assays were carried out using an iTaq universal SYBR green supermix (Bio-Rad) with specific primers (Suppl. Materials and Methods). The PCR reaction was performed using the CFX Real-Time PCR system (Bio-Rad). Relative fold change of gene expression was calculated using the $2^{-\Delta\Delta Ct}$ method [116] with the standard errors of the mean from 4 independently conducted experiments using the *rpsJ* gene as a comparator [117]. The induction folds were tested for statistical significance using the Kolmogorov-Smirnov test for normality,

Friedman's ANOVA to compare treated and untreated conditions, and Bonferroni-Dunn's method for multiple comparisons between the gene of interest and comparator (Suppl. Materials and Methods).

CRediT authorship contribution statement

Matthew Phanchana: Conceptualization, Data curation, Formal analysis, Funding acquisition, Investigation, Project administration, Supervision, Writing – review & editing. **Wannarat Chanket:** Conceptualization, Formal analysis, Investigation, Visualization, Writing – original draft. **Apiwat Sangphukieo:** Data curation, Formal analysis, Investigation, Writing – review & editing. **Methinee Pipatthana:** Conceptualization, Funding acquisition, Resources, Visualization, Writing – review & editing. **Surang Chankhamhaengdecha:** Conceptualization, Funding acquisition, Resources, Writing – review & editing. **Phurt Harnvoravongchai:** Conceptualization, Funding acquisition, Resources, Writing – review & editing. **Tavan Janvilisri:** Conceptualization, Funding acquisition, Project administration, Resources, Supervision, Writing – review & editing.

Declaration of Generative AI and AI-assisted technologies in the writing process

During the preparation of this work the authors used ChatGPT and QuillBot in order to improve readability and edit grammatical errors. After using these tools, the authors reviewed and edited the content as needed and take full responsibility for the content of the publication.

Declaration of Competing Interest

The authors declare the following financial interests/personal relationships which may be considered as potential competing interests: Matthew Phanchana reports financial support was provided by Mahidol University. Matthew Phanchana, Methinee Pipatthana, Phurt Harnvoravongchai, Surang Chankhamhaengdecha, Tavan Janvilisri reports financial support was provided by National Research Council of Thailand. Wannarat Chanket reports financial support was provided by Development and Promotion of Science and Technology Talents Project. Tavan Janvilisri is an Editorial Board Member for Scientific Reports, Experimental and Therapeutic Medicine, Molecular Medicine Reports, World Journal of Biological Chemistry, and ScienceAsia, and was not involved in the editorial review or the decision to publish this article. If there are other authors, they declare that they have no known competing financial interests or personal relationships that could have appeared to influence the work reported in this paper.

Acknowledgements

This research project is supported by Mahidol University to Matthew Phanchana (NDFR 07/2564) and the East Asia Science and Innovation Area Joint Research Program (e-ASIA JRP) through the National Research Council of Thailand (NRCT; N11A670792). Wannarat Chanket is supported by the Development and Promotion of Science and Technology Talents Project (DPST). We would like to thank Kathryn Fisher for critically reading the manuscript.

Appendix A. Supporting information

Supplementary data associated with this article can be found in the online version at doi:10.1016/j.csbj.2024.05.027.

References

[1] Alshrari AS, Hudu SA, Elmigdadi F, Imran Mohd. The urgent threat of *Clostridioides difficile* infection: a glimpse of the drugs of the future, with related patents and prospects. Biomedicines 2023;11(2).

[2] Buddle JE, Fagan RP. Pathogenicity and virulence of *Clostridioides difficile*. Virulence 2023;14(1):2150452.

[3] Leffler DA, Lamont JT. Clostridium difficile infection. United States: The New England Journal of Medicine; 2015. p. 287–8.

[4] Abughanimeh Omar, Qasrawi Ayman, Kaddourah Osama, Momani Laith Al, Abu Ghanimeh Mouhanna. *Clostridium difficile* infection in oncology patients: epidemiology, pathophysiology, risk factors, diagnosis, and treatment (Available from) Hosp Pr [Internet] 2018;46(5):266–77. https://doi.org/10.1080/21548331.2018.1533673.

[5] Saleh MM, Petri Jr WA. Type 3 immunity during *Clostridioides difficile* infection: too much of a good thing? Infect Immun 2019;88(1):e00306–19.

[6] MHLP Souza, Melo-Filho AA, MFG Rocha, Lyerly DM, Cunha FQ, AAM Lima, et al. The involvement of macrophage-derived tumour necrosis factor and lipoxygenase products on the neutrophil recruitment induced by *Clostridium difficile* toxin B. Immunology [Internet], 91; 1997. p. 281–8. Available from: https://onlinelibrary.wiley.com/doi/abs/10.1046/j.1365-2567.1997.00243.x.

[7] McDonald LC, Gerding DN, Johnson S, Bakken JS, Carroll KC, Coffin SE, et al. Clinical practice guidelines for *Clostridium difficile* infection in adults and children: 2017 update by the Infectious Diseases Society of America (IDSA) and Society for Healthcare Epidemiology of America (SHEA). Clin Infect Dis 2018;66(7). e1–48.

[8] Johnson S, Lavergne V, Skinner AM, Gonzales-Luna AJ, Garey KW, Kelly CP, et al. Clinical Practice Guideline by the Infectious Diseases Society of America (IDSA) and Society for Healthcare Epidemiology of America (SHEA): 2021 Focused Update Guidelines on Management of *Clostridioides difficile* Infection in Adults. e1029–44. Available from Clin Infect Dis [Internet] 2021;73(5). https://doi.org/10.1093/cid/ciab549.

[9] Harnvoravongchai P., Pipatthana M., Chankhamhaengdecha S., Janvilisri T. Insights into drug resistance mechanisms in *Clostridium difficile*. Venter H, editor. Essays Biochem. 2017 Mar 3;61(1):81–8.

[10] Wilcox MH, Gerding DN, Poxton IR, Kelly C, Nathan R, Birch T, et al. Bezlotoxumab for prevention of recurrent *Clostridium difficile* Infection. N Engl J Med 2017;376(4):305–17.

[11] Giacobbe DR, Dettori S, Di Bella S, Vena A, Granata G, Luzzati R, et al. Bezlotoxumab for preventing recurrent *Clostridioides difficile* infection: a narrative review from pathophysiology to clinical studies. Infect Dis Ther 2020;9(3):481–94.

[12] Thandavaram A, Channar A, Purohit A, Shrestha B, Patel D, Shah H, et al. The efficacy of Bezlotoxumab in the prevention of recurrent *Clostridium difficile*: a systematic review. Cureus 2022;14(8):e27979.

[13] de la Villa S, Herrero S, Muñoz P, Rodríguez C, Valerio M, Reigadas E, et al. Real-world use of bezlotoxumab and fecal microbiota transplantation for the treatment of *Clostridioides difficile* infection. Open Forum Infect Dis 2023;10(2):ofad028.

[14] Ooijevaar RE, van Beurden YH, Terveer EM, Goorhuis A, Bauer MP, Keller JJ, et al. Update of treatment algorithms for *Clostridium difficile* infection. Clin Microbiol Infect [Internet] 2018;24(5):452–62 (Available from), ⟨https://www.sciencedirect.com/science/article/pii/S1198743X18300211⟩.

[15] Phanchana M, Harnvoravongchai P, Wongkuna S, Phetruen T, Phothichaisri W, Panturat S, et al. Frontiers in antibiotic alternatives for *Clostridioides difficile* infection. World J Gastroenterol 2021;27(42):7210–32.

[16] Du D, Wang-Kan X, Neuberger A, van Veen HW, Pos KM, Piddock LJV, et al. Multidrug efflux pumps: structure, function and regulation. Nat Rev Microbiol 2018;16(9):523–39.

[17] Hernando-Amado S, Blanco P, Alcalde-Rico M, Corona F, Reales-Calderón JA, Sánchez MB, et al. Multidrug efflux pumps as main players in intrinsic and acquired resistance to antimicrobials. Drug Resist Updat 2016;28:13–27.

[18] Ngernsombat C, Sreesai S, Harnvoravongchai P, Chankhamhaengdecha S, Janvilisri T. CD2068 potentially mediates multidrug efflux in *Clostridium difficile*. Sci Rep 2017;7(1):9982.

[19] Pipatthana M, Harnvoravongchai P, Pongchaikul P, Likhitrattanapisal S, Phanchana M, Chankhamhaengdecha S, et al. The repertoire of ABC proteins in *Clostridioides difficile*. Comput Struct Biotechnol J [Internet] 2021;19:2905–20 (Available from), ⟨https://www.sciencedirect.com/science/article/pii/S2001037021001938⟩.

[20] Teelucksingh T, Thompson LK, Cox G, Margolin W. The evolutionary conservation of *Escherichia coli* drug efflux pumps supports physiological functions. J Bacteriol 2020;202(22). e00367-20.

[21] Delmar JA, Yu EW. The AbgT family: a novel class of antimetabolite transporters. Protein Sci 2016;25(2):322–37.

[22] Hassan KA, Liu Q, Elbourne LDH, Ahmad I, Sharples D, Naidu V, et al. Pacing across the membrane: the novel PACE family of efflux pumps is widespread in Gram-negative pathogens. Res Microbiol 2018;169(7):450–4.

[23] Plé C, Tam HK, Vieira Da Cruz A, Compagne N, Jiménez-Castellanos JC, Müller RT, et al. Pyridylpiperazine-based allosteric inhibitors of RND-type multidrug efflux pumps. Nat Commun 2022;13(1):115.

[24] Ying L, Xizhen G. Role of berberine as a potential efflux pump inhibitor against MdfA from *Escherichia coli*: in vitro and in silico studies. Microbiol Spectr 2023;0(0). e03324-22.

[25] Zahmatkesh H, Mirpour M, Zamani H, Rasti B. Effect of samarium oxide nanoparticles fabricated by curcumin on efflux pump and virulence genes expression in MDR *Pseudomonas aeruginosa* and *Staphylococcus aureus*. J Clust Sci 2022.

[26] Elbourne LDH, Tetu SG, Hassan KA, Paulsen IT. TransportDB 2.0: a database for exploring membrane transporters in sequenced genomes from all domains of life. Nucleic Acids Res 2017;45(D1):D320–4.

[27] Schindler BD, Kaatz GW. Multidrug efflux pumps of Gram-positive bacteria. Drug Resist Updat 2016;27:1–13.

[28] Bailey TL, Johnson J, Grant CE, Noble WS. The MEME Suite. W39–49. Available from Nucleic Acids Res [Internet] 2015;43(W1). https://doi.org/10.1093/nar/gkv416.

[29] Krogh A, Larsson B, von Heijne G, Sonnhammer ELL. Predicting transmembrane protein topology with a hidden markov model: application to complete genomes. J Mol Biol [Internet] 2001;305(3):567–80 (Available from), ⟨https://www.sciencedirect.com/science/article/pii/S0022283600943158⟩.

[30] Hallgren J., Tsirigos K., Pedersen M.D., Almagro Armenteros J.J., Marcatili P., Nielsen H., et al. DeepTMHMM predicts alpha and beta transmembrane proteins using deep neural networks. bioRxiv; 2022.

[31] Hirokawa T, Boon-Chieng S, Mitaku S. SOSUI: classification and secondary structure prediction system for membrane proteins (Available from) Bioinforma [Internet] 1998;14(4):378–9. https://doi.org/10.1093/bioinformatics/14.4.378.

[32] Mistry J, Chuguransky S, Williams L, Qureshi M, Salazar GA, Sonnhammer ELL, et al. Pfam: The protein families database in 2021. Nucleic Acids Res 2021;49(D1):D412–9.

[33] Paysan-Lafosse T, Blum M, Chuguransky S, Grego T, Pinto BL, Salazar GA, et al. Inter 2022 Nucleic Acids Res 2023;(D1):D418–27.

[34] Saier Jr MH, Reddy VS, Tamang DG, Västermark Å. The transporter classification database. D251–8. Available from Nucleic Acids Res [Internet] 2014 Jan 1;42(D1). https://doi.org/10.1093/nar/gkt1097.

[35] Katoh K, Standley DM. MAFFT multiple sequence alignment software version 7: improvements in performance and usability. Mol Biol Evol 2013 Apr 1;30(4):772–80.

[36] Guindon S, Dufayard JF, Lefort V, Anisimova M, Hordijk W, Gascuel O. New algorithms and methods to estimate maximum-likelihood phylogenies: assessing the performance of PhyML 3.0. Syst Biol 2010;59(3):307–21.

[37] Lefort V, Longueville JE, Gascuel O. SMS: smart model selection in PhyML. Mol Biol Evol 2017;34(9):2422–4.

[38] Jumper J, Evans R, Pritzel A, Green T, Figurnov M, Ronneberger O, et al. Highly accurate protein structure prediction with AlphaFold. Nature 2021;596(7873):583–9.

[39] Holm L. Dali server: structural unification of protein families. Nucleic Acids Res 2022;50(W1):W210–5.

[40] Boudker O, Verdon G. Structural perspectives on secondary active transporters. Trends Pharm Sci [Internet] 2010;31(9):418–26 (Available from), ⟨https://www.sciencedirect.com/science/article/pii/S0165614710001100⟩.

[41] Padan E. Bacterial membrane transport: secondary transport proteins. In: Encyclopedia of Life Sciences [Internet]. 2019. p. 1–13. Available from: https://doi.org/10.1002/9780470015902.a0003743.pub3.

[42] Emerson JE, Stabler RA, Wren BW, Fairweather NF. Microarray analysis of the transcriptional responses of *Clostridium difficile* to environmental and antibiotic stress. J Med Microbiol 2008;57(Pt 6):757–64.

[43] Janvilisri T, Scaria J, Chang YF. Transcriptional profiling of *Clostridium difficile* and Caco-2 cells during infection. J Infect Dis 2010;202(2):282–90.

[44] Ternan NG, Jain S, Srivastava M, McMullan G. Comparative transcriptional analysis of clinically relevant heat stress response in *Clostridium difficile* strain 630. PLoS One 2012;7(7):1–10.

[45] Dembek M, Stabler RA, Witney AA, Wren BW, Fairweather NF. Transcriptional analysis of temporal gene expression in germinating *Clostridium difficile* 630 endospores. PLoS One 2013;8(5):1–12.

[46] Yılmaz Ç, Özcengiz G. Antibiotics: pharmacokinetics, toxicity, resistance and multidrug efflux pumps. Biochem Pharm [Internet] 2017;133:43–62 (Available from), ⟨https://www.sciencedirect.com/science/article/pii/S0006295216303513⟩.

[47] Blanco P, Hernando-Amado S, Reales-Calderon JA, Corona F, Lira F, Alcalde-Rico M, et al. Bacterial multidrug efflux pumps: much more than antibiotic resistance determinants. Microorg [Internet] 2016;4(1) (Available from), ⟨https://www.mdpi.com/2076-2607/4/1/14⟩.

[48] Sandler N, Keynan A. Cell wall synthesis and initiation of deoxyribonucleic acid replication in *Bacillus subtilis*. J Bacteriol [Internet], 148; 1981. p. 443–9. Available from: https://journals.asm.org/doi/abs/10.1128/jb.148.2.443-449.1981.

[49] Hammes WP, Neuhaus FC. On the mechanism of action of vancomycin: inhibition of peptidoglycan synthesis in *Gaffkya homari*. Antimicrob Agents Chemother [Internet], 6; 1974. p. 722–8. Available from: https://journals.asm.org/doi/abs/10.1128/aac.6.6.722.

[50] Müller M. Mode of action of metronidazole on anaerobic bacteria and protozoa. Surg [Internet] 1983;93(1):165–71 (Available from), ⟨https://www.surgjournal.com/article/0039-6060(83)90295-7/abstract⟩.

[51] Tenson T, Lovmar M, Ehrenberg M. The mechanism of action of macrolides, lincosamides and streptogramin B reveals the nascent peptide exit path in the ribosome. J Mol Biol [Internet] 2003;330(5):1005–14 (Available from), ⟨https://www.sciencedirect.com/science/article/pii/S0022283603006624⟩.

[52] Venugopal AA, Johnson S. Fidaxomicin: a novel macrocyclic antibiotic approved for treatment of *Clostridium difficile* infection (Available from) Clin Infect Dis [Internet] 2012;54(4):568–74. https://doi.org/10.1093/cid/cir830.

[53] Aldred KJ, Kerns RJ, Osheroff N. Mechanism of quinolone action and resistance (Available from) Biochem [Internet] 2014;53(10):1565–74. https://doi.org/10.1021/bi5000564.

[54] Bhatt S, Chatterjee S. Fluoroquinolone antibiotics: occurrence, mode of action, resistance, environmental detection, and remediation – a comprehensive review. Environ Pollut [Internet] 2022;315:120440 (Available from), ⟨https://www.sciencedirect.com/science/article/pii/S0269749122016542⟩.

[55] Sebaihia M, Wren BW, Mullany P, Fairweather NF, Minton N, Stabler R, et al. The multidrug-resistant human pathogen *Clostridium difficile* has a highly mobile, mosaic genome. Nat Genet 2006;38(7):779–86.

[56] Lebel S, Bouttier S, Lambert T. The cme gene of *Clostridium difficile* confers multidrug resistance in Enterococcus faecalis. FEMS Microbiol Lett 2004 Sep;238(1):93–100.

[57] Dridi L, Tankovic J, Petit JC. CdeA of *Clostridium difficile*, a new multidrug efflux transporter of the MATE family. Micro Drug Resist 2004;10(3):191–6.

[58] Claxton DP, Jagessar KL, Mchaourab HS. Principles of alternating access in multidrug and toxin extrusion (MATE) transporters. J Mol Biol [Internet] 2021;433(16):166959 (Available from), ⟨https://www.sciencedirect.com/science/article/pii/S0022283621001601⟩.

[59] Krah A, Huber RG, Zachariae U, Bond PJ. On the ion coupling mechanism of the MATE transporter ClbM. Biochimica et Biophysica Acta (BBA). Biomembr [Internet] 2020;1862(2):183137 (Available from), ⟨https://www.sciencedirect.com/science/article/pii/S0005273619302858⟩.

[60] Kim J, Cater RJ, Choy BC, Mancia F. Structural insights into transporter-mediated drug resistance in infectious diseases. J Mol Biol [Internet] 2021;433(16):167005 (Available from), ⟨https://www.sciencedirect.com/science/article/pii/S0022283621002060⟩.

[61] Jack DL, Yang NM H, Saier Jr M. The drug/metabolite transporter superfamily (Available from) Eur J Biochem [Internet] 2001;268(13):3620–39. https://doi.org/10.1046/j.1432-1327.2001.02265.x.

[62] Cerasi M, Liu JZ, Ammendola S, Poe AJ, Petrarca P, Pesciaroli M, et al. The ZupT transporter plays an important role in zinc homeostasis and contributes to *Salmonella enterica* virulence (Available from) Met [Internet] 2014;6(4):845–53. https://doi.org/10.1039/c3mt00352c.

[63] Quan G, Xia P, Lian S, Wu Y, Zhu G. Zinc uptake system ZnuACB is essential for maintaining pathogenic phenotype of F4ac+ enterotoxigenic *E. coli* (ETEC) under a zinc restricted environment (Available from) Vet Res [Internet] 2020;51(1):127. https://doi.org/10.1186/s13567-020-00854-1.

[64] Berges M, Michel AM, Lassek C, Nuss AM, Beckstette M, Dersch P, et al. Iron regulation in *Clostridioides difficile*. Front Microbiol [Internet] 2018;9. Available from: https://www.frontiersin.org/articles/10.3389/fmicb.2018.03183.

[65] Kanehisa M, Furumichi M, Sato Y, Kawashima M, Ishiguro-Watanabe M. KEGG for taxonomy-based analysis of pathways and genomes (Available from) Nucleic Acids Res [Internet] 2023;51(D1):D587–92. https://doi.org/10.1093/nar/gkac963.

[66] Du D, Wang Z, James NR, Voss JE, Klimont E, Ohene-Agyei T, et al. Structure of the AcrAB-TolC multidrug efflux pump. Nature 2014 May;509(7501):512–5.

[67] Burley SK, Bhikadiya C, Bi C, Bittrich S, Chao H, Chen L, et al. RCSB Protein Data Bank (RCSB.org): delivery of experimentally-determined PDB structures alongside one million computed structure models of proteins from artificial intelligence/machine learning (Available from) Nucleic Acids Res [Internet] 2023;51(D1):D488–508. https://doi.org/10.1093/nar/gkac1077.

[68] Meng EC, Pettersen EF, Couch GS, Huang CC, Ferrin TE. Tools for integrated sequence-structure analysis with UCSF Chimera (Available from) BMC Bioinforma [Internet] 2006;7(1):339. https://doi.org/10.1186/1471-2105-7-339.

[69] Meng EC, Goddard TD, Pettersen EF, Couch GS, Pearson ZJ, Morris JH, et al. UCSF ChimeraX: tools for structure building and analysis (Available from) Protein Sci [Internet] 2023;32(11):e4792. https://doi.org/10.1002/pro.4792.

[70] Wang Z., Fan G., Hryc C.F., Blaza J.N., Serysheva I.I., Schmid M.F., et al. An allosteric transport mechanism for the AcrAB-TolC multidrug efflux pump. Boudker O, editor. Elife. 2017;6:e24905.

[71] Su CC, Bolla JR, Kumar N, Radhakrishnan A, Long F, Delmar JA, et al. Structure and function of *Neisseria gonorrhoeae* MtrF illuminates a class of antimetabolite efflux pumps. Cell Rep [Internet] 2015;11(1):61–70 (Available from), ⟨https://www.sciencedirect.com/science/article/pii/S2211124715002454⟩.

[72] Engevik MA, Morra CN, Röth D, Engevik K, Spinler JK, Devaraj S, et al. Microbial metabolic capacity for intestinal folate production and modulation of host folate receptors. Front Microbiol [Internet] 2019. 10. Available from: https://www.frontiersin.org/articles/10.3389/fmicb.2019.02305.

[73] Bolla JR, Su CC, Delmar JA, Radhakrishnan A, Kumar N, Chou TH, et al. Crystal structure of the *Alcanivorax borkumensis* YdaH transporter reveals an unusual topology. Nat Commun 2015;6:6874.

[74] Shome S, Sankar K, Jernigan RL. Simulated drug efflux for the AbgT family of membrane transporters (Available from) J Chem Inf Model [Internet] 2021;61(11):5673–81. https://doi.org/10.1021/acs.jcim.1c00516.

[75] Zhong P, Dazhi J, Bum KH, SC W, Bin W, Yi-Wei T, et al. Update on antimicrobial resistance in *Clostridium difficile*: resistance mechanisms and antimicrobial susceptibility testing. J Clin Microbiol 2017;55(7):1998–2008.

[76] Wickramage I, Spigaglia P, Sun X. Mechanisms of antibiotic resistance of *Clostridioides difficile*. J Antimicrob Chemother 2021;76(12):3077–90.

[77] O'Grady K, Knight DR, Riley TV. Antimicrobial resistance in *Clostridioides difficile*. Eur J Clin Microbiol Infect Dis 2021;40(12):2459–78.

[78] Sawada R, Ke R, Tsuji T, Sonoyama M, Mitaku S. Ratio of membrane proteins in total proteomes of prokaryota. Biophys (Oxf) 2007;3:37–45.

[79] Pedro AQ, Queiroz JA, Passarinha LA. Smoothing membrane protein structure determination by initial upstream stage improvements (Available from) Appl Microbiol Biotechnol [Internet] 2019;103(14):5483–500. https://doi.org/10.1007/s00253-019-09873-1.

[80] Pagès JM, James CE, Winterhalter M. The porin and the permeating antibiotic: a selective diffusion barrier in Gram-negative bacteria. Nat Rev Microbiol 2008 Dec;6(12):893–903.

[81] Nikaido H. Structure and mechanism of RND-type multidrug efflux pumps. Adv Enzym Relat Areas Mol Biol 2011;77:1–60.
[82] Malik AJ, Poole AM, Allison JR. Structural phylogenetics with confidence (Available from) Mol Biol Evol [Internet] 2020;37(9):2711–26. https://doi.org/10.1093/molbev/msaa100.
[83] AlphaFold and beyond. Nat Methods [Internet] 2023;20(2):163. https://doi.org/10.1038/s41592-023-01790-6.
[84] Barrio-Hernandez I, Yeo J, Jänes J, Mirdita M, Gilchrist CLM, Wein T, et al. Clustering predicted structures at the scale of the known protein universe (Available from) Nat [Internet] 2023. https://doi.org/10.1038/s41586-023-06510-w.
[85] Durairaj J, Waterhouse AM, Mets T, Brodiazhenko T, Abdullah M, Studer G, et al. Uncovering new families and folds in the natural protein universe (Available from) Nat [Internet] 2023. https://doi.org/10.1038/s41586-023-06622-3.
[86] Hoda A, Tafaj M, Sallaku E. In silico structural, functional and phylogenetic analyses of cellulase from *Ruminococcus albus*. J Genet Eng Biotechnol [Internet] 2021;19(1):58. https://doi.org/10.1186/s43141-021-00162-x.
[87] Bayly-Jones C, Whisstock JC. Mining folded proteomes in the era of accurate structure prediction. PLoS Comput Biol [Internet] 2022;18(3):e1009930. -. Available from: https://doi.org/10.1371/journal.pcbi.1009930.
[88] Hajieghrari B, Niazi A. Phylogenetic and evolutionary analysis of plant small RNA 2'-O-methyltransferase (HEN1) protein family. J Mol Evol [Internet] 2023;91(4):424–40 (Available from), ⟨http://europepmc.org/abstract/MED/37191719⟩.
[89] Dar D, Shamir M, Mellin JR, Koutero M, Stern-Ginossar N, Cossart P, et al. Term-seq reveals abundant ribo-regulation of antibiotics resistance in bacteria. Sci (1979) [Internet] 2016;352(6282):aad9822 (Available from), ⟨https://www.science.org/doi/abs/10.1126/science.aad9822⟩.
[90] Rowan-Nash AD, Korry BJ, Mylonakis E, Belenky P. Cross-domain and viral interactions in the microbiome. Microbiology and Molecular Biology Reviews [Internet], 83; 2019. p. e00044–18 (Available from), ⟨https://journals.asm.org/doi/abs/10.1128/MMBR.00044-18⟩.
[91] Zgurskaya HI, Malloci G, Chandar B, Vargiu AV, Ruggerone P. Bacterial efflux transporters' polyspecificity – a gift and a curse? Curr Opin Microbiol [Internet] 2021;61:115–23 (Available from), ⟨https://www.sciencedirect.com/science/article/pii/S136952742100045X⟩.
[92] Huang L, Wu C, Gao H, Xu C, Dai M, Huang L, et al. Bacterial multidrug efflux pumps at the frontline of antimicrobial resistance: an overview. Antibiot [Internet] 2022;11(4) (Available from), ⟨https://www.mdpi.com/2079-6382/11/4/520⟩.
[93] Venter H, Mowla R, Ohene-Agyei T, Ma S. RND-type drug efflux pumps from gram-negative bacteria: molecular mechanism and inhibition. Front Microbiol [Internet] 2015;6. Available from: https://www.frontiersin.org/articles/10.3389/fmicb.2015.00377.
[94] Dong N, Zeng Y, Wang Y, Liu C, Lu J, Cai C, et al. Distribution and spread of the mobilised RND efflux pump gene cluster *tmexCD-toprJ* in clinical gram-negative bacteria: a molecular epidemiological study (Available from) Lancet Microbe [Internet] 2022;3(11):e846–56. https://doi.org/10.1016/S2666-5247(22)00221-X.
[95] Arkowitz RA, Wickner W. SecD and SecF are required for the proton electrochemical gradient stimulation of preprotein translocation. EMBO J [Internet] 1994;13(4):954–63 (Available from, http://europepmc.org/abstract/MED/8112309.
[96] Saier MHJ, Paulsen IT. Phylogeny of multidrug transporters. Semin Cell Dev Biol 2001;12(3):205–13.
[97] Gupta RS. Origin of diderm (Gram-negative) bacteria: antibiotic selection pressure rather than endosymbiosis likely led to the evolution of bacterial cells with two membranes (Available from) Antonie Van Leeuwenhoek [Internet] 2011;100(2):171–82. https://doi.org/10.1007/s10482-011-9616-8.
[98] Megrian D, Taib N, Witwinowski J, Beloin C, Gribaldo S. One or two membranes? diderm Firmicutes challenge the Gram-positive/Gram-negative divide (Available from) Mol Microbiol [Internet] 2020;113(3):659–71. https://doi.org/10.1111/mmi.14469.
[99] Muñoz-Gómez SA, Roger AJ. Leaving negative ancestors behind (Available from) Elife [Internet] 2016;5:e20061. https://doi.org/10.7554/eLife.20061.
[100] Taib N, Megrian D, Witwinowski J, Adam P, Poppleton D, Borrel G, et al. Genome-wide analysis of the Firmicutes illuminates the diderm/monoderm transition (Available from) Nat Ecol Evol [Internet] 2020;4(12):1661–72. https://doi.org/10.1038/s41559-020-01299-7.
[101] Lopez J.M.E. Characterization of an efflux pump system, the CD_AcrA-AcrB-TolC complex, in *Clostridium difficile* [Thesis]. Kansas State University; 2017.
[102] Partridge Sally R, Kwong Stephen M, Neville Firth, Jensen Slade O. Mobile genetic elements associated with antimicrobial resistance. Clin Microbiol Rev [Internet] 2018;31(4). 10.1128/cmr.00088-17. Available from: https://doi.org/10.1128/cmr.00088-17.
[103] Piddock LJV. Clinically relevant chromosomally encoded multidrug resistance efflux pumps in bacteria (Available from) Clin Microbiol Rev [Internet] 2006 Apr 1;19(2):382–402. https://doi.org/10.1128/cmr.19.2.382-402.2006.
[104] Teelucksingh T, Thompson LK, Zhu S, Kuehfuss NM, Goetz JA, Gilbert SE, et al. A genetic platform to investigate the functions of bacterial drug efflux pumps. Nat Chem Biol [Internet] 2022;18(12):1399–409 (Available from), http://europepmc.org/abstract/MED/36065018.
[105] Luchao L, Miao W, Chengzhen W, Xun G, Qiwen Y, PS R, et al. Emergence of a plasmid-encoded Resistance-Nodulation-Division efflux pump conferring resistance to multiple drugs, including tigecycline, in *Klebsiella pneumoniae*. mBio [Internet] 2020;11(2). 10.1128/mbio.02930-19. Available from: https://doi.org/10.1128/mbio.02930-19.
[106] Whelan FJ, Hall RJ, McInerney JO. Evidence for selection in the abundant accessory gene content of a prokaryote pangenome (Available from) Mol Biol Evol [Internet] 2021 Sep 1;38(9):3697–708. https://doi.org/10.1093/molbev/msab139.
[107] Duval M, Dar D, Carvalho F, Rocha EPC, Sorek R. Cossart P. HflXr, a homolog of a ribosome-splitting factor, mediates antibiotic resistance. Proc Natl Acad Sci USA 2018;115(52):13359–64.
[108] Perrin E, Fondi M, Papaleo MC, Maida I, Buroni S, Pasca MR, et al. Exploring the HME and HAE1 efflux systems in the genus *Burkholderia* (Available from) BMC Evol Biol [Internet] 2010;10(1):164. https://doi.org/10.1186/1471-2148-10-164.
[109] Górecki K, McEvoy MM. Phylogenetic analysis reveals an ancient gene duplication as the origin of the MdtABC efflux pump (-. Available from) PLoS One [Internet] 2020;15(2):e0228877. https://doi.org/10.1371/journal.pone.0228877.
[110] Sanchez-Herrero JF, Bernabeu M, Prieto A, Hüttener M, Juárez A. Gene duplications in the genomes of *Staphylococci* and *Enterococci*. Front Mol Biosci [Internet] 2020;7. Available from: https://www.frontiersin.org/articles/10.3389/fmolb.2020.00160.
[111] Donati C, Hiller NL, Tettelin H, Muzzi A, Croucher NJ, Angiuoli SV, et al. Structure and dynamics of the pan-genome of *Streptococcus pneumoniae* and closely related species (Available from) Genome Biol [Internet] 2010;11(10):R107. https://doi.org/10.1186/gb-2010-11-10-r107.
[112] Mosquera-Rendón J, Rada-Bravo AM, Cárdenas-Brito S, Corredor M, Restrepo-Pineda E, Benítez-Páez A. Pangenome-wide and molecular evolution analyses of the *Pseudomonas aeruginosa* species (Available from) BMC Genom [Internet] 2016;17(1):45. https://doi.org/10.1186/s12864-016-2364-4.
[113] Anisimova M, Gil M, Dufayard JF, Dessimoz C, Gascuel O. Survey of branch support methods demonstrates accuracy, power, and robustness of fast likelihood-based approximation schemes. Syst Biol 2011;60(5):685–99.
[114] Martí-Solans J., Børve A., Bump P., Hejnol A., Lynagh T. Peripheral and central employment of acid-sensing ion channels during early bilaterian evolution. Tessmar-Raible K, Aldrich RW, editors. Elife. 2023;12:e81613.
[115] Chaudhari NM, Gupta VK, Dutta C. BPGA- an ultra-fast pan-genome analysis pipeline (Available from) Sci Rep [Internet] 2016;6(1):24373. https://doi.org/10.1038/srep24373.
[116] Rao X, Huang X, Zhou Z, Lin X. An improvement of the 2(-delta delta CT) method for quantitative real-time polymerase chain reaction data analysis. Biostat Bioinforma Biomath 2013;3(3):71–85.
[117] Metcalf D, Sharif S, Weese JS. Evaluation of candidate reference genes in *Clostridium difficile* for gene expression normalization. Anaerobe 2010 Aug;16(4):439–43.
[118] Saier MH. Molecular phylogeny as a basis for the classification of transport proteins from bacteria, archaea and eukarya. In: Poole RK, editor. Advances in Microbial Physiology [Internet]. Academic Press; 1998. p. 81–136 (Available from), ⟨https://www.sciencedirect.com/science/article/pii/S0065291108601307⟩.
[119] Anes J, McCusker MP, Fanning S, Martins M. The ins and outs of RND efflux pumps in *Escherichia coli*. Front Microbiol [Internet] 2015;6. Available from: https://www.frontiersin.org/articles/10.3389/fmicb.2015.00587.